COUPLING FROM POINTS ON AN AIRCRAFT STRUCTURE TO AIRCRAFT ANTENNA TERMINALS

Harold W. Jesse

79

COUPLING FROM POINTS
ON AN AIRCRAFT STRUCTURE
TO AIRCRAFT ANTENNA TERMINALS

* * * * *

Harold W. Jesse

COUPLING FROM POINTS
ON AN AIRCRAFT STRUCTURE
TO AIRCRAFT ANTENNA TERMINALS

by

Harold W. Jesse

Lieutenant, United States Navy

Submitted in partial fulfillment of
the requirements for the degree of

MASTER OF SCIENCE
IN
ENGINEERING ELECTRONICS

United States Naval Postgraduate School
Monterey, California

1 9 5 7

Thesis
J477

COUPLING FROM POINTS

ON AN AIRCRAFT STRUCTURE

TO AIRCRAFT ANTENNA TERMINALS

by

Harold W. Jesse

This work is accepted as fulfilling

the thesis requirements for the degree of

MASTER OF SCIENCE

IN

ENGINEERING ELECTRONICS

from the

United States Naval Postgraduate School

ABSTRACT

The problem of precipitation static has long been of concern to aviation personnel. A need has been expressed for knowing the coupling of a current pulse from various parts of the aircraft structure to the antenna terminals. A system for making these measurements is devised and results of the measurements for an A3D type aircraft outlined.

The major portion of the work was accomplished at Stanford Research Institute, Menlo Park, California. The author is indebted to the personnel of Stanford Research Institute for their cooperation during the project, in particular to Dr. R. L. Tanner for his invaluable guidance and direction and to G. R. Hilbers and J. E. Nanevicz for their assistance and suggestions.

Acknowledgements are also due to Professors J. G. Chaney and J. B. Turner of the United States Naval Postgraduate School for their assistance and encouragement in this investigation.

TABLE OF CONTENTS

LIST OF ILLUSTRATIONS

Figure		Page

CHAPTER I

INTRODUCTION

1. History.

Radio interference caused by what is now commonly known as precipitation static has been experienced for many years. The first recorded instances were in ground radio stations during periods of very intense precipitation. Several good descriptions of this phenomena as experienced in ground and shipborne installations have been written.[1,2] Since precipitation static occurred only rarely in ground stations with the result of lowering the efficiency of communications during these periods, and since the effect was not a hazard to equipment or personnel, there was no incentive for intensive research into the problem until precipitation static was encountered during aircraft flights.

In the early 1930's the amount of flying during instrument weather by military and commercial aircraft increased substantially. These aircraft were dependent upon electronic communication and navigation equipment for safety of flight. Since precipitation static could cause loss of communication and navigation information from low frequency radio ranges for periods of several hours, it became a definite hazard. The problem began to receive serious attention as pilots complained of the

difficulties caused by precipitation static and as aircraft were lost in accidents believed caused by the pilot losing orientation and not having any effective communications.

At that time the theory of the cause of precipitation static that received the most widespread acceptance was that advanced by Curtis in 1914 as a result of Marriot's article.[3] Curtis stated that the probable cause of precipitation static was charged particles striking the antenna structure. On the basis of this hypothesis the shielded loop antenna was introduced in 1935. This offered considerable improvement over the open wire antennas that were in use previous to its introduction,[4] and on the basis of tests run by Transcontinental and Western Airlines, the Department of Commerce ordered all commercial carriers to equip their aircraft with the shielded loop by October, 1937.

The fact, that in spite of shielding the loop and thereby preventing the charged particles from striking the antenna there were still periods of communication loss due to precipitation static, showed that there was some other mechanism responsible for at least a part of the noise. It is now believed that the improvement of the shielded loop over the open wire antenna is due to the shield preventing corona discharges on the antenna structure itself, and that the antenna is electrostatically

shielded from noise sources. Further exploration of the problem was done during a series of flight tests from November, 1936 to June, 1937. The program was conducted by Reed College, Purdue University, Oregon State College, Bendix Radio Corporation, Bell Telephone Laboratories, and United Airlines.[5] The results of the investigation as reported by Hucke made the significant conclusion that the principal cause of precipitation static was not charged particles striking the antenna but rather was due to corona discharge from the antenna itself or from other extremities of the aircraft. Hucke lists seven different ways by which he believed the aircraft became charged, stressing particularly the transfer of charge from charged particles that strike the aircraft structure in flight. As another result of Hucke's investigation, the trailing wire dischargers came into use. This consisted of a high resistance in series with the discharge point utilizing the electric field about the charged aircraft to move charges away from the aircraft.

During World War II and the period thereafter quite a bit of work was done in studying the precipitation static problem. The largest project was the joint Army-Navy Project at Minneapolis in 1946 under the direction of Dr. Ross Gunn.[6] An extensive program was conducted of both actual flight tests and utilizing a

B-17 suspended in a hanger and charged by a high voltage source until the plane broke into corona. The group tested several of the methods for reduction of precipitation static that had been suggested. As a result of the program the wick discharger and dielectric coated antenna were suggested as the best and most practical answers in sight at that time. The wick discharger is simply a fiber wick which gives a bundle of very fine discharge points at the end. This causes the corona discharge to occur at relatively low potentials giving corona pulses of lower amplitude and higher frequency. The dielectric coated antenna prevents the antenna itself from breaking into corona, thereby eliminating the corona pulses from the point of maximum coupling.

Other work was done during the war on understanding the basic mechanism of precipitation static and suggesting methods of overcoming the problem. Among these were the group under Huggins at Oregon State College.[7] They studied the pulse shape of positive point corona by investigating the frequency spectrum of noise voltages and from them determing the Fourier transform of the corona pulses. They also studied the reduction of initiation voltage for corona by use of a small oxy-acetylene flame. Toward the end of the war a group under Dr. Irving Langmuir at General Electric Corporation undertook an extensive study of the fundamental phenomena

of precipitation static.[8,9] They showed that the major source of precipitation static was definitely corona discharge and that the aircraft charging was due to triboelectric effect between ice particles and aircraft surfaces rather than transfer of charge as theorized by Hucke. This was later confirmed by the Minneapolis group under Gunn. Other results of Langmuir's investigation were that aircraft surfaces should be bare rather than painted aluminum, that the magnitude of currents was space charge limited, and that corona current should be a linear function of airspeed. Another method of reducing precipitation static was the "block and squirter" discharge system proposed by Dr. H. J. Dana of Washington State University.[10] This system forced corona discharge from high potential points to occur by use of high audio frequency potentials of the order of 100KV. The discharge occurred on alternate half cycles during which the receiver was blanked. The receiver was unblanked during the quiet half cycles for reception of the desired signal.

In 1948 Bennett proposed a discharger consisting of a high potential probe within a cylindrical collar.[11] The probe was to be maintained 5-10 KV negative with respect to the aircraft and a wind stream allowed to pass through the cylinder. This design was based partially on the conclusion of Beach that a sharp tip is a better discharger than a wick.[12] Beach's conclusions have

since been shown false,[16] and Bennett's proposed discharger has never been flight tested.

In 1950 Philco Corporation reported on a biased ionic discharger with multiple points and on a coaxial needle point and cylinder.[13] A voltage to induce corona was established between the point and the cylinder. The high intensity field near the point would tend to capture ions of opposite charge while like charge would be swept away by the airstream. In evaluating these devices, Bartelt at W.A.D.C. showed that about thirty coaxial dischargers would be needed to maintain zero field on a 150 knot aircraft with a 500 microamp charging current.[14] Since charging rate increases roughly as the cube of the airspeed this system would become inadequate at the higher speeds commonly encountered. In 1953 Cornell Aeronautical Laboratory built a corona point discharger with the output controlled by field intensity meters.[15] They calculated that a net discharge current of one milliampere should result from 100 KV applied to the corona points. Tests yielded short term transients of the order of 400 microamperes with 35 KV applied, however this was not blow away current since there was not a corresponding change in the field intensity.

The work of Dr. R. L. Tanner at Stanford Research Institute as reported in 1953 contributed significantly to the understanding of precipitation static processes.[16]

He obtained the first accurate oscillographic pictures of corona pulses, determining the Laplace transform therefrom; and showed how the pulse varied as a function of discharge point radius, pressure, and voltage. He also determined the spatial extent of the discharge current, which is important since the noise signals are dependent upon the dipole moment of the discharge current. He also derived a basic coupling of the corona pulse to the receiver terminals. On the basis of his work he concluded that the noise could be reduced either by reducing the pulse size or by reducing the coupling between the discharge and the receiver.

In 1956 Harlor, Jordan, and Murcray at Denver Research Institute reported on their investigations into different types of dischargers.[19] They experimented with fuel additives to increase the natural discharging capabilities of engine exhaust gases. They also investigated the use of flame, electron gun tube, and hot wire thermionic emitter type dischargers.

2. The Basis of Precipitation Static.

As has been shown in the history the main cause of precipitation static is corona discharge from the extremities of the aircraft.[3,6,8,16] The corona occurs when the aircraft is charged to a high potential by triboelectric charging.[6,9,16] This occurs when ice particles and water droplets present in clouds strike

the aircraft and in rubbing along the surface leave a charge in the same way as a glass rod becomes charged when rubbed with a piece of fur. This theory explains the high charging rate of aircraft. This could not be justified by the supposition of Hucke that charge was obtained by transfer from charged particles striking the aircraft. It is known that aircraft charge at a much higher rate than that which would occur if all the charge from particles through which they flew were transferred to them, and cases have even been reported where the aircraft acquired a negative charge while flying through positively charged precipitation particles.[8] The triboelectric charging theory also explains why aircraft are always charged negatively since substances with a low dielectric constant acquire a negative charge when rubbed with a substance having a higher dielectric charge. On the basis of this, the Army-Navy Project at Minneapolis tried to find surface coatings for the aircraft to reduce the charge.[6] This proved unsuccessful in that the coatings would soon wear off and the oil and grease naturally present around aircraft would film over the coating and destroy its effectiveness.

As the aircraft enters the region of precipitation, the triboelectric charging soon raises the aircraft to a potential of several hundred thousand volts or more.

As the aircraft charges a highly concentrated field forms at the extremities of the aircraft and at any sharp points or projections on the surface. Eventually the field builds up high enough to cause the points to break into negative point corona. After the corona pulse the field builds back up again until another corona pulse occurs. The corona pulses have a pulse width of the order of .1 microsecond, a rise time of the order of .01 microsecond, and occur at a rate dependent upon the voltage and the radius of the discharge point.[16] The pulses couple electromagnetically to the antenna thereby giving the noise signal which blanks the desired signal. The pulse form is very similar to

$$i = 1.14\,a e^{-.0091t} - 1.56\,a e^{-.117t} \cos(.129t - .0375)$$

where a is the peak magnitude of the pulse.[16] By obtaining the frequency transform it can be shown that the frequency spectrum starts to fall off at about 1 mc and is down about 36 db at 30 mc, thereby showing why precipitation static is a problem only below the vhf band.

In addition to the autogenous charging of the aircraft due to the triboelectric effect, precipitation static can also be caused by exogenous charging. This occurs when the aircraft flies between two highly charged clouds of opposite polarity and this induces high field concentrations on the aircraft causing corona to occur.

This effect is of little concern since it takes place only for short periods of time. Another effect is the noise due to streamer discharges from dielectric surfaces.[18] The discarded original theory that precipitation static was caused by charged particles striking the antenna has since been found to be of some concern in that significant noise voltages are produced by this effect at the lower frequencies.

3. Scope of Investigation.

At the present time the problem of precipitation static still exists and is becoming a more significant problem as aircraft speeds increase. The most promising fields of endeavor to eliminate the problem appear to be continued work in the design, development, and test of discharge devices; and the problem of locating the discharger in the best spot on the aircraft for minimizing coupling to the aircraft radio antennas.

The purpose of this investigation is to devise a system of measuring the coupling to the antenna from the various points of the aircraft as a function of frequency. The system is designed for use in a scaled down model of an aircraft so that the measurements can be made on a tower away from ground and other reflecting surfaces. It is felt that these measurements will aid in the locating of the dischargers so as to reduce coupling to the antenna to a minimum and as an aid in the design of new types of

dischargers which depend upon the fields present. For some types of aircraft the possibility exists that the coupling to the antenna from all normal discharge points is comparatively low for a certain frequency band. If so it might be possible to designate a frequency in this band for use as the normal air ground frequency or as a standby or alternate frequency if this does not conflict with other frequency allocations.

The measurements will also allow the computation of antenna terminal short circuit current for a discharge current pulse located at any position on the aircraft. This will then enable computation of receiver response to the corona discharge pulse and hence possibly aid in the understanding of the problem of precipitation static.

CHAPTER II

THE BASIC COUPLING THEOREM

The noise produced at the antenna terminals by a corona discharge at some point on the aircraft structure depends directly upon the coupling between that point and the antenna terminals. In order to evaluate the coupling a mathematical relationship between the discharge and the antenna terminals must be developed. This has been done by Tanner in his report, "Radio Interference from Corona Discharges."[16] Since this is an electromagnetic problem, it can best be approached by utilizing Maxwell's equations.

The problem can be solved most generally by utilizing any arbitrary shape as in Fig. 1. The two regions of interest are T_1 representing the volume removed from the conducting body to form the antenna terminals, and T_2, representing the volume external to the conducting body in which charge moves during a discharge. Quantities pertaining to the two regions will be identified by the subscripts 1 and 2.

In order to derive the coupling relation it is necessary to consider two separate and independent situations as follows:

Situation I - A voltage V_1 is applied at the antenna terminals causing a field $\bar{E}^I$ to be produced

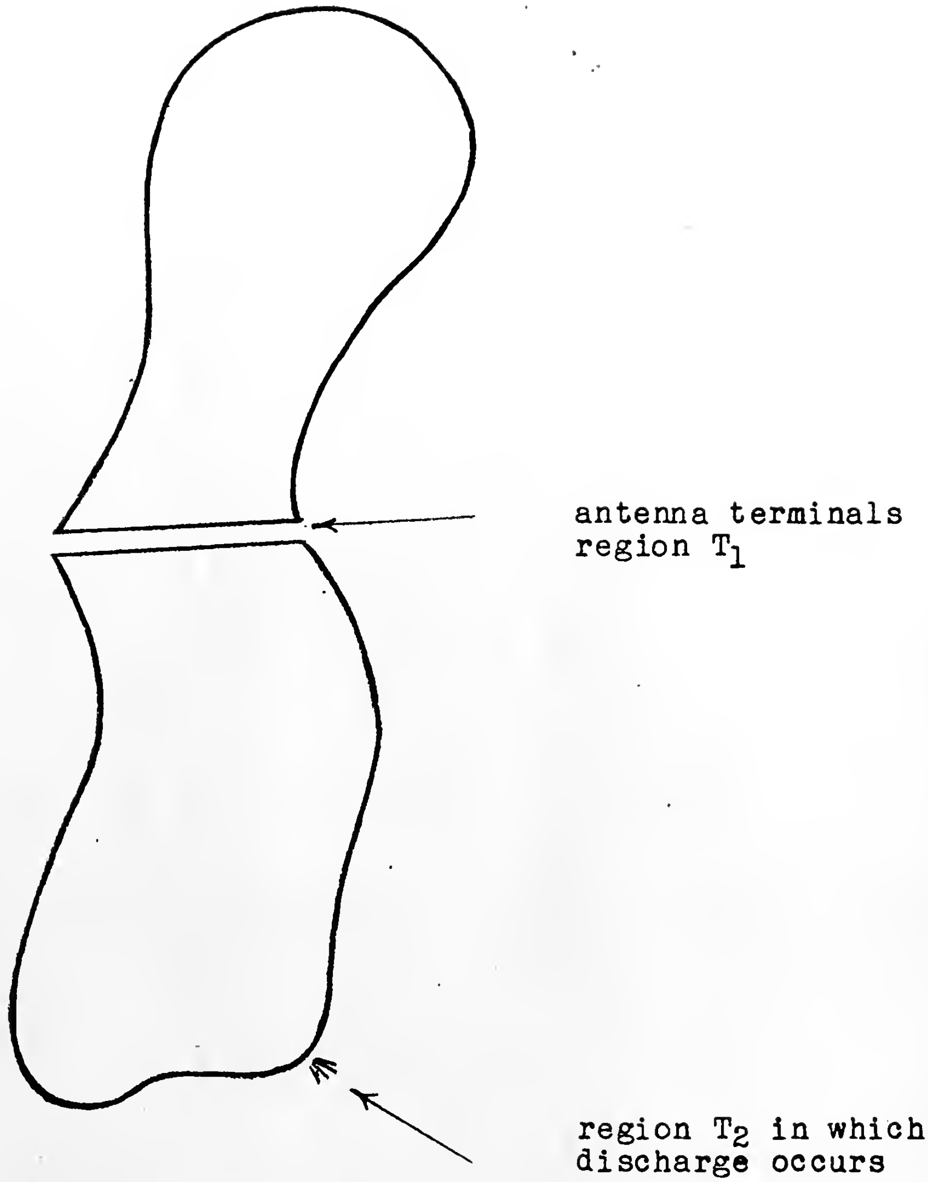

FIG. 1

COUPLING FROM A DISCHARGE ON A CONDUCTING BODY TO THE ANTENNA TERMINALS

everywhere in space and of particular interest in region T_2.

Situation II - Charge moves in region T_2 (a finite current density $\bar{J}^{II}$ in region T_2) in response to which a voltage V_1^{II} is produced at the antenna terminals.

For each of the cases we can write Maxwell's equations relating $\bar{E}$, $\bar{H}$, and $\bar{J}$.

$$\nabla \times \bar{E} = -j\omega\mu\bar{H} \tag{1}$$

$$\nabla \times \bar{H} = j\omega\epsilon\bar{E}' + \bar{J} \tag{2}$$

The quantity

$$\bar{E}^{I} \times \bar{H}^{II} - \bar{E}^{II} \times \bar{H}^{I}$$

can be formed and the divergence theorem applied giving

$$\oint (\bar{E}^{I} \times \bar{H}^{II} - \bar{E}^{II} \times \bar{H}^{I}) \cdot d\bar{S} = \int \nabla \cdot (\bar{E}^{I} \times \bar{H}^{II} - E^{II} \times \bar{H}^{I})\, dv \tag{3}$$

The volume integral of Eq. 3 can be changed by vector identity to

$$\int (\bar{H}^{II} \cdot \nabla \times \bar{E}^{I} - \bar{E}^{I} \cdot \nabla \times \bar{H}^{II} - \bar{H}^{I} \cdot \nabla \times \bar{E}^{II} + \bar{E}^{II} \cdot \nabla \times \bar{H}^{I})\, dV$$

Substituting Eqs. (1) and (2) we have

$$\int (-\bar{H}^{II} \cdot j\omega\mu\bar{H}^{I} - \bar{E}^{I} \cdot j\omega\epsilon\bar{E}^{II} - \bar{E}^{II} \cdot \bar{J}^{I} + \bar{H}^{I} \cdot j\omega\mu\bar{H}^{II} + \bar{E}^{II} \cdot j\omega\epsilon\bar{E}^{I} + \bar{E}^{I} \cdot \bar{J}^{II})\, dv$$

which reduces simply to

$$\int (\bar{E}^{I} \cdot \bar{J}^{II} - \bar{E}^{II} \cdot \bar{J}^{I})\, dv$$

and Eq. (3) now becomes

$$\oint (\bar{E}^{I} \times \bar{H}^{II} - \bar{E}^{II} \times \bar{H}^{I}) \cdot \overline{dS} = \int (\bar{E}^{I} \cdot \bar{J}^{II} - \bar{E}^{II} \cdot \bar{J}^{I})\, dv \qquad (4)$$

From the divergence theorem it is known that the volume included in the volume integral is that which is bounded by the surface integral. Since the region of interest is all space external to the conductors of Fig. 1 including the regions T_1 and T_2, it can be seen that the surface integral of concern is that of the surface of the conductors and the surface at infinity.

Sommerfeld's radiation condition makes the surface integral from the surface at infinity equal to zero.[20] Assuming a perfect conductor the boundry conditions on the surface of the conductors insure that the vector $\bar{E} \times \bar{H}$ will lie in a plane tangent to the surface while the element of area $\overline{dS}$ is normal to the surface. The vectors $\bar{E} \times \bar{H}$ and $\overline{dS}$ are therefore orthogonal and the surface integral in equation (4) is identically equal to zero.

Equation (4) can therefore be written

$$\int \bar{E}^{II} \cdot \bar{J}^{I} dv = \int \bar{E}^{I} \cdot \bar{J}^{II} dv \qquad (5)$$

From the conditions for cases I and II previously specified it can be seen that the left hand side of Eq. (5) applies to the volume of the antenna terminals while the right hand side applies to the volume in which the discharge occurs. Eq. (5) therefore becomes

$$\int_{T_1} \bar{E}^{II} \cdot \bar{J}^{I} dv = \int_{T_2} \bar{E}^{I} \cdot \bar{J}^{II} dv \qquad (6)$$

The left hand side of Eq. (6) can be defined as the product $V_1^{II} I_1^{I}$ and the equation rearranged to give one form of the basic coupling theorem

$$V_1^{II} = \frac{1}{I_1^{I}} \int_{T_2} \bar{E}^{I} \cdot \bar{J}^{II} dv \qquad (7)$$

A more useful form of the theorem can be obtained, by dividing both sides of Eq. (7) by the antenna terminal impedance Z_{11}. The left hand side thus becomes the open circuit voltage at the terminals caused by the discharge divided by the antenna impedance; or from Thevenin's theorem, the short circuit current produced by the discharge, I_1^{II}. The product $I_1^{I} Z_{11}$ is simply V_1^{I}, and therefore equation (7) becomes

$$I_1^{II} = \frac{1}{V_1^{I}} \int_{T_2} \bar{E}^{I} \cdot \bar{J}^{II} dv \qquad (8)$$

From Eq. (8), the short circuit current at the antenna terminals can easily be determined if the space and time distribution of current density during the discharge is known and if the electric field produced in the region of the discharge by a voltage applied to the antenna terminals can be determined. With this information and conventional circuit theory, the response of a receiver connected to the antenna terminals can be computed. Conversely if the short circuit current at the antenna terminals is known and the electric field in the vicinity of the discharge is known then Eq. (8) can be used as an integral equation for determining the current distribution of the discharge.

CHAPTER III

THE SYSTEM FOR MEASUREMENT OF THE COUPLING FACTOR

The coupling theorem derived in Chapter II shows the dependence of the short circuit current upon the current distribution of the discharge, the antenna terminal voltage, and the field configuration in the vicinity of the discharge. Tanner has shown that the spatial extent of corona discharge pulses is very small and that over the region of the discharge the electric field is essentially constant.[16] The fact that $\overline{E}^I$ can be considered constant over the region T_2 enables it to be brought out from the integral of Eq. (8) leaving the short circuit current dependent upon the current distribution of the discharge pulse times a constant factor E^I/V_1^I which will henceforth be referred to as the coupling function, ψ.

The space and time distribution of the discharge pulses has been quite extensively investigated, however little is known about the magnitude of the coupling function, ψ , outside of the obvious conclusions that the coupling function would be expected to be greater at a point of high field concentration such as the wing tip than at a point of low field concentration such as the wing root.

In order to measure ψ some method of injecting a signal at the point of interest on the fuselage must be developed, and a method of measuring the strength of the received signal at the antenna terminals must be devised. To complete the requirements for the basic system there is the need for some type of standard field configuration for which the coupling function can be computed since the measurements at the antenna terminals will only give the relative coupling of one point with respect to another.

There is also the further requirement that nothing in the system alter the normal field configuration in the vicinity of the aircraft. Any conducting material close to the aircraft will cause the fields to change. This imposes the requirement that the aircraft under investigation be raised above the surface of the earth, that there be no external power cords to the model to operate equipment, and that the signal source be non-conductive.

A block diagram of the system developed is shown in Fig. 2 and a photograph of the arrangement of equipment in Fig. 3. The reasons for the choice of system and components will be given later. Basic operation is as follows with the numbers in parenthesis referring to Fig. 3. The high voltage d.c. power supply, (1), is the driving source for the spark gap signal generator

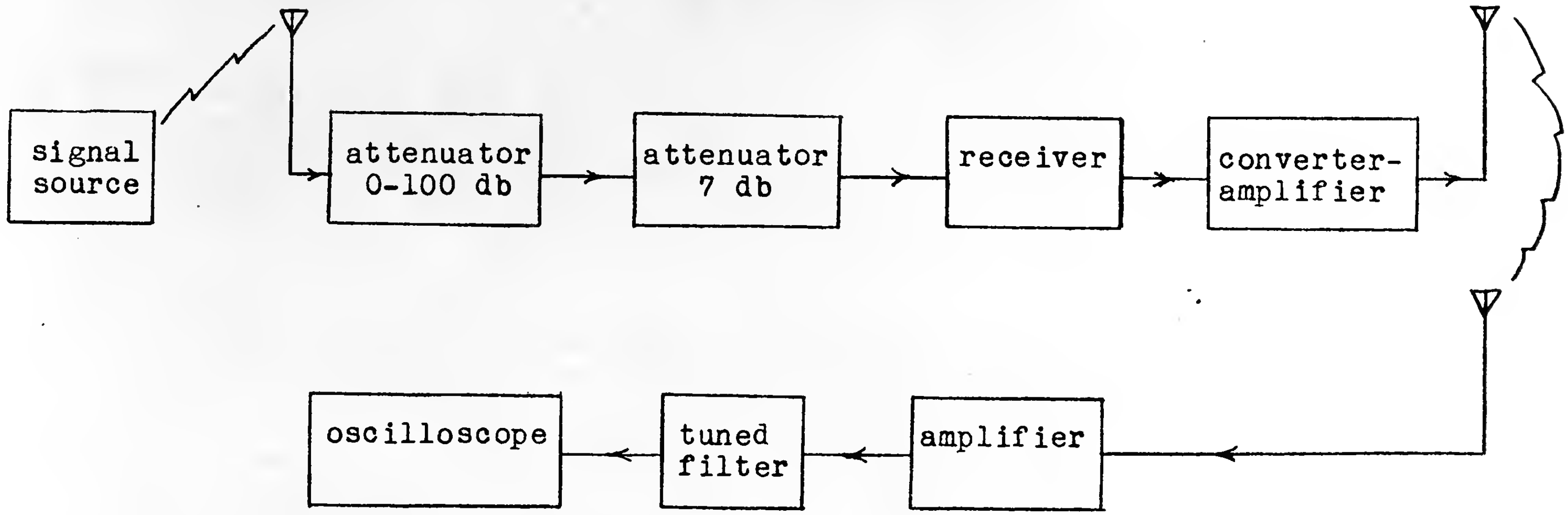

FIG. 2

BLOCK DIAGRAM OF THE COUPLING MEASUREMENT SYSTEM

FIG. 3

THE MEASUREMENT SYSTEM

C19810

probe, (2). Connection from the power supply to the end of the signal generator probe was made through RG8/U cable with the outer shield removed to lower the chance of breakdown through the insulation causing extraneous signals. The bank of resistors, (3), totaling 1000 megohms is placed in the system as a personnel safety feature. The signal at the antenna terminals, (4), is passed through a variable 0-100 db Daven attenuator and another Daven attenuator with a fixed seven db of attenuation to prevent reflections and thence to a communications receiver. The system was connected with 50 ohm cable throughout to maintain a matched system. The signal from the final I.F. amplifier of the receiver was reduced in frequency through a converter-amplifier and transmitted to a remote location for observation. The attenuators, receiver, and converter were contained within the model and power obtained from 6 volt storage batteries and a Mallory VP554H Vibrapack. The telemetered signal was received at the antenna, (5), passed through a Donner Video Probe Model 60 Amplifier, (8), and a tuned circuit filter, (7), and then displayed on a Techtronix Model 535 Oscilloscope, (8).

In order to made this type of measurement several possibilities immediately suggest themselves for a transmitting device. First; a signal generator could be carried internally in the model and the signal radiated

by an antenna placed through a hole in the aircraft structure at the point in question and the received signal measured at the antenna terminals. Second; the principle of reciprocity could be used, the signal being applied at the normal aircraft antenna terminals and the radiated signal being picked up by an antenna at the point in question and fed internally through the model to the received signal measuring device. The third possibility is to have either the signal source or the receiving-measuring device located externally on the model at the point in question. There are also the further requirements for all three possibilities that the signal radiating device or receiving-measuring device located at the point in question be small so that the signal source will be effectively very small and hence the coupling measured will be that from a very small area, and also any conducting material external to the aircraft structure be kept at an absolute minimum size so as to minimize field distortions.

After consideration the first two possibilities were discarded because of antenna efficiency and mechanical problems. In order to meet the requirements of essentially point source and small conductor the antenna used would have to be essentially an infinitesimal dipole type antenna. Since the frequencies in question are low this would be a highly inefficient radiator and would require

quite a considerable amount of power from the signal source. The natural radiation from the signal source and the transmission line internally in the model would be of the same order of magnitude or greater than that from the antenna. Since both the signal source and the receiver would be internally carried in the model this would impose severe shielding problems in order to insure that the signal being measured by the receiver was actually that from the antenna terminals and not including any signal voltage induced in the receiver by direct pickup from the source. Varing the position of the antenna from point to point would impose time consuming problems due to the small spaces in which connections would have to be made to the antenna. Another difficulty is that the areas of interest are the trailing edges of the wing and tail structures which are very thin, and drilling holes for the antenna would alter the natural fields to some extent.

In approaching the problem from the standpoint of the third possibility listed, the problem was how to obtain a signal generator of infinitesimal size that contained its own power supply. This immediately ruled out any conventional type tuned oscillator and limited the possibility to some type of broad band noise source where the required frequency selection would have to be accomplished at the receiver.

The most practical way to obtain such a source appears to be a spark gap. The mechanism of spark discharges has been thoroughly investigated by Loeb.[21,22] He shows how the frequency spectrum of a spark would make it suitable for the desired measurements and what factors affect the gap breakdown voltage and hence the signal output.

The source used is shown in Fig. 4 with construction details shown in Fig. 5. The measurement system as first envisioned appeared to require as large a signal as possible, and hence some details of construction appear which are not essential to operation as finally used. The gap itself was made of two small 3/16 inch diameter polished steel ball bearings. One ball was kept at ground potential by making contact with the aircraft structure through the 3/64 inch screw. The aircraft model was maintained at ground potential by connecting it to the ground side of the power supply by means of a high resistance lead. The other ball was connected to the high voltage side of the power supply by means of high voltage cable to the end of the spark gap signal generator probe and thence internally through the probe on high resistance lead to the ball. The high resistance lead was made by painting nylon rod with very high resistance paint. The high resistance lead is such that

FIG. 4 ILLUSTRATING PLACEMENT OF SIGNAL PROBE AND ATTENUATOR CONTROLS

C19808

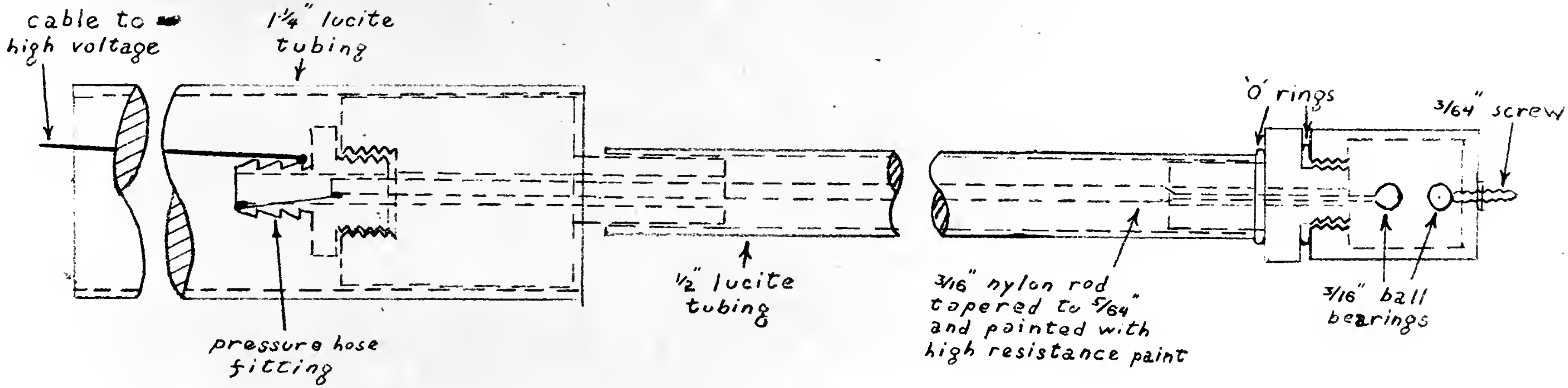

FIG. 5

SPARK GAP SIGNAL GENERATOR PROBE

27

its presence in the vicinity of the aircraft does not distort the natural fields close to the aircraft structure since it will not support an a.c. wave down its length.

The high voltage supply used is shown in Fig. 6. It is a continuously variable supply delivering from zero to 150 KV d.c. The protective resistance bank can also be seen enclosed in polyfoam to prevent arc over to the stand or corona and hence extraneous signals.

When the high voltage ball bearing electrode charges up to the gap breakdown voltage, the electron avalanche of the spark discharge discharges the ball, causing a pulse of energy to be radiated. The ball then charges up again to breakdown thereby causing a series of pulses to be formed. The pulses were observed on a Techtronix 545 oscilloscope by placing the spark between two metal plates spaced four cm. apart and taking the signal from the plates across a 50 ohm resistor. The pulses observed had a pulse width of approximately .05 microseconds which was very possibly due to the response of the oscilloscope, with very short rise time which shows the broad band characteristics of the signal spectrum. The pulse amplitude depended upon the breakdown voltage of the gap which in turn was a function mainly of the spacing of the balls and the pressure in the gap. A pulse amplitude of 26 volts was obtained using a d.c. supply of about 120 KV and a

FIG. 6

HIGH VOLTAGE SUPPLY AND PROTECTIVE RESISTOR BANK

C19809

pressure of about 100 p.s.i. This magnitude signal was not required for the measurements and an amplitude of about 2.5 volts was used with the gap at atmospheric pressure and a voltage supply of about 60 KV, which was higher than the voltage required for breakdown with the gap spacing used.

While the gap did not have to be enclosed for pressure purposes, the enclosure helped keep dust and other foreign particles from being attracted to the balls and varying the pulse amplitude or even quenching the spark. Even after being enclosed the spark gap electrodes had to be removed and cleaned after several hours of operation to remove oxidation from the balls which would eventually cause erratic operation of the gap.

The system imposed no other requirements on the pulse spectrum other than that there be sufficient signal components at all the frequencies of interest. The spectrum was roughly checked by measuring a receiver response using a calibrated signal generator, and comparing it to the response measured using the spark gap as the signal source. The spectrum was found to be essentially flat up to 120 mcs., the highest frequency checked, so therefore the spark gap was quite suitable for use as the signal source.

The other major component of the system is the receiver-converter-amplifier combination. The requirement

for the receiver was only that it have a linear response to signal amplitude over a very small range, since the attenuator was used to make all signals approximately the same amplitude prior to the receiver. There was no requirement for knowing the receiver frequency response or having an accurately calibrated gain, or even having a constant gain as will be shown later. The main criterion for selecting the receiver to be used was, "would it fit into the model?" The receiver selected was a National Model HFS Communications Receiver which had been converted from a regenerative IF to a straight superhetrodyne receiver and the AGC circuit disabled. The receiver and its power supply were internally mounted in the model as shown in Fig. 7.

The output from the final IF amplifier of the receiver at 10.7 mcs was fed to the converter amplifier, Fig. 9, where it was converted to approximately 1.6 mcs and then further amplified for transmission. A circuit diagram of the converter-amplifier is shown in Fig. 8.

Fig. 9 also shows connection from the converter-amplifier to the telemetering transmitting antenna shown in full in Fig. 10, which consisted of shunt feeding a wing section by a long wire attached near the end of the wing and tuning with a variable capacitor between the base of the wire and a point near the wing root.

FIG. 7

RECEIVER LOCATION IN AIRCRAFT [illegible]

C19807

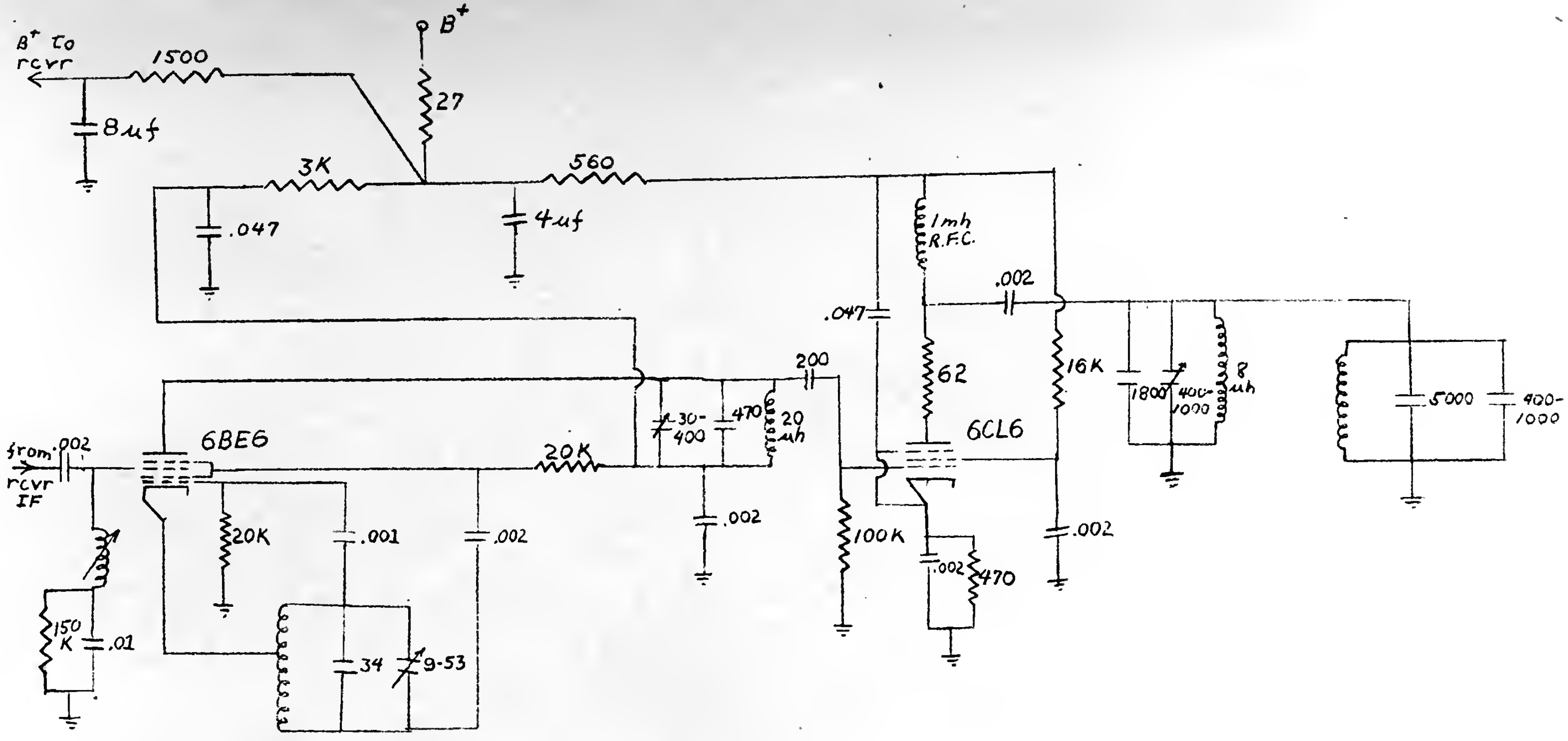

FIG. 8

CIRCUIT DIAGRAM OF CONVERTER AMPLIFIER

FIG. 9

CONVERTER AMPLIFIER

C19812

FIG. 10

TELEMETERING TRANSMITTING ANTENNA

C198813

Fig. 11 shows the telemetering system receiving antenna which is a balanced tuned loop made from RG8/U cable. The signal is transformer coupled to the amplifier shown in Fig. 11. The amplifier is a unity gain device which is inserted to provide isolation between the tuned antenna circuit and a tuned filter circuit prior to the oscilloscope.

The filter functions mainly to increase the selectivity to the oscilloscope so that interference from adjacent broadcast and navigation stations and light fixture and machinery noises which are picked up by the tuned loop will be reduced to a minimum when the signal is viewed on the scope.

In making the measurements the receiver was tuned to a known frequency. The signal probe was then inserted between the plates of the standard field and the signal taken from across a 50 ohm resistor and fed into the system at the input side of the variable attenuator. The signal amplitude on the oscilloscope was adjusted to give a deflection of approximately .2 volts by means of the attenuator which can be seen mounted on the side of the aircraft model in Fig. 9. The attenuator was then disconnected from the standard field and connected to the antenna terminals. The signal generator probe was then placed on one of the points of interest on the aircraft structure, and measurements again made as before

FIG. 11

TELEMETERING RECEIVING ANTENNA AND IF [illegible]

C19811

and attenuator setting and scope deflection recorded. Readings were taken for all of the other points similarly and recorded. The first or reference point was checked several times during each frequency run to insure that some parameter of the system such as signal strength or receiver gain did not change. The standard field reading was rechecked as the last reading on each frequency run.

In order to obtain the coupling function from the data obtained, the resultant amplitudes of the various points and the standard field were computed from the combination of oscilloscope and attenuator readings. The amplitude of the standard field, h_s, needed also to be divided by two since the reading was taken from across a 50 ohm resistor and fed into the 50 ohm system; while the amplitude for the points on the aircraft model, h_p, were taken from the antenna terminals, which had a fairly high capacitive reactance, and were then fed into the 50 ohm system.

A relative coupling can now be easily found by simply dividing h_p by h_s for all of the points of interest and for each of the frequencies taken in the frequency range of interest. While the relative coupling is of interest, much more information can be gained from the absolute coupling factor; since then all that is necessary to apply Eq. (8) to find the antenna terminal short circuit current is the current distribution of the discharge pulse. The

ratio of coupling functions will be equal to the ratio of the amplitudes measured, or referring to the standard field

$$\frac{\psi}{\psi_s} = \frac{h_p}{h_s} \qquad (9)$$

The presence of the two small ball bearings between two parallel plates would not cause the field set up between the plates to vary appreciably from the standard field configuration, inversely proportional to the distance between the plates, d, if the balls are close to the mid-plane between the plates and if the space occupied by the balls is much smaller than d. For the standard and signal probe used this was not the case, however, since one plate was connected to one of the balls thru the short screw at the tip of the probe, and also since the spark gap took up an appreciable part of the distance between the plates.

In order to correct this difficulty another spark gap and wider spaced standard field plates were utilized. The spark gap consisted of two small ball bearings mounted off the end of a flat plastic plate. High voltage and ground connections were made to the balls through high resistance leads painted on the sides of the plate. Several readings of both standard field and aircraft point amplitudes were made at different frequencies. The readings for the standard field were made with the gap centered between the plates which were spaced 10 cm apart, and the readings for the aircraft structure points were made with the center

of the gap one inch behind the point in question and orientated so that the discharge would be normal to the aircraft surface at the point.

By again finding the ratio of h_p to h_s we can find the absolute coupling factor, ψ , since coupling for the standard field, ψ_s , is now known. This type of signal probe is much more difficult to position and hold steady during the reading than the other, but it can be used for a representative number of readings for comparison in order to obtain a correction factor for the original probe to correct to a standard 1/d field.

Readings were made and a mean correction factor of 1.7 obtained by comparing h_p/h_s for the second signal probe to that of the first probe. Correction factor varied from extremes of 1.0 to 2.3 with the majority between 1.5 and 2.0 yeilding the mean value of 1.7.

The absolute coupling factor can be now found from applying Eq. (9), by multiplying the h_p/h_s ratio by the correction factor 1.7, and by the standard field coupling factor, 1/d or .1 cm $^{-1}$. The value thus computed will be the coupling factor of a discharge current at a point one inch behind the given point on the aircraft structure.

CHAPTER IV

COMPILATION OF RESULTS OF THE MEASUREMENTS

The apparatus as described in Chapter III was assembled for making coupling measurements on a fifth scale model of an A3D or B-66 type aircraft. The frequencies measured would have to be similarly scaled, and the receiver range utilized of 18 to 115 mcs would correspond to a range of 3.6 to 23 mcs on a full scale aircraft.

The measurements were made for the points on the structure as shown in Fig. 12. Coupling was measured for corresponding points on both the starboard and port horizontal stabilizers at a frequency in the midrange and was found to be identical, verifying the expected symmetry.

In Fig. 13 the values of coupling for the points on the horizontal stabilizer are plotted as a function of frequency. The points all have the same general type curve as would be expected in a cylindrical antenna as you varied position along the antenna. The variation of point A is probably due to its proximity to the fuselage and vertical stabilizer structures.

The dips and peaks of the curves are due to resonance effects on the airframe. It would be difficult to find the cause of each irregularity, however reasonable

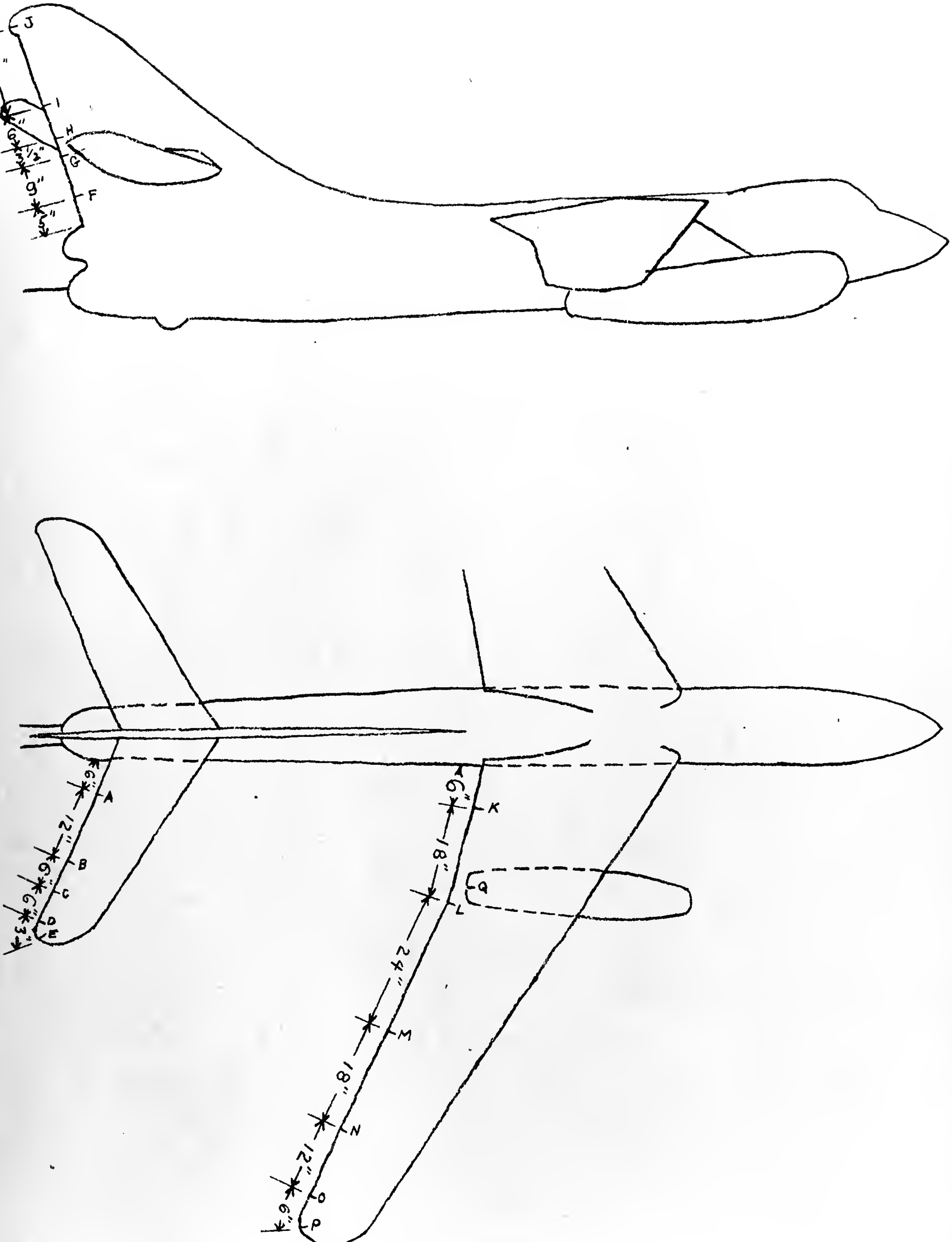

FIG. 12

LOCATION OF MEASUREMENT POINTS ON FIFTH

SCALE B-66 MODEL

FIG. 13

THE COUPLING FUNCTION AS A FUNCTION OF FREQUENCY FOR POINTS ON THE HORIZONTAL STABILIZER

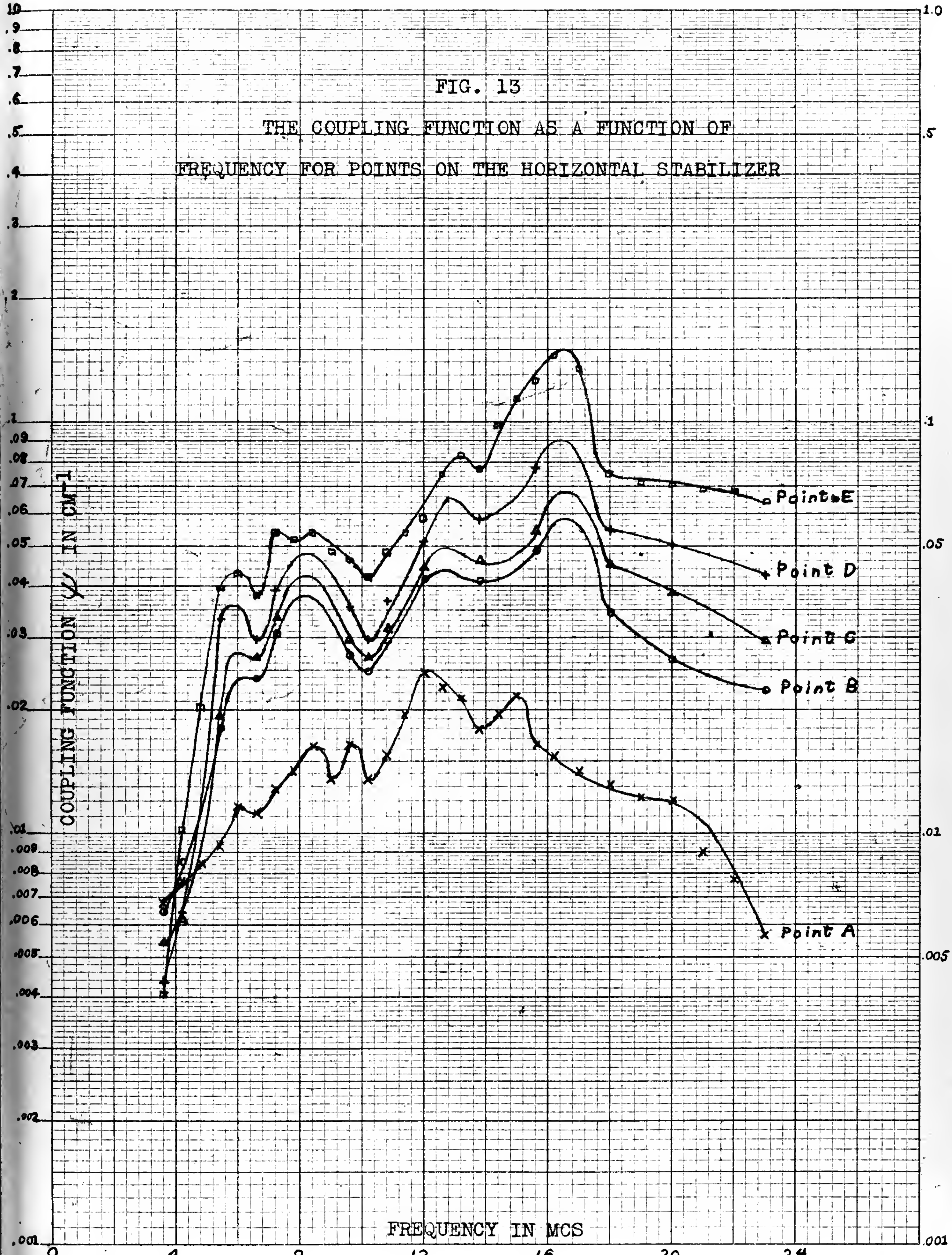

assumptions as to the reasons for the major peaks can be made.

The simplest antenna configuration resembling a tail cap antenna that can be treated mathematically is the assymetric dipole. Assuming the short leg of the dipole short with comparison to a wavelength, Tanner has shown that the coupling from the end of the long element would have a major peak when the length of the long element was approximately a half wave length, with smaller peaks as the element passes through succeeding half wave lengths.[16]

While no exact analogy can be made, one would expect to find similar half wave peaks from points on the aircraft with variations due to resonance effects of other portions of the structure. For the A3D the first half wave length to the wing tip would be at about 7.5 mcs.

The peaks on the curves of Fig. 13 at about 8 mcs are probably due to the half wave resonance while the large peaks about 16.5 mcs are probably caused by a combination of full wave length to the wing tip at 15 mcs and half wave length from the antenna terminals to the tip of the horizontal stabilizer at 18 mcs.

The coupling for the vertical stabilizer is shown in Fig. 14. Coupling from point J should correspond to that from the end of the short element of the asymmetric dipole. The dipole coupling is fairly constant

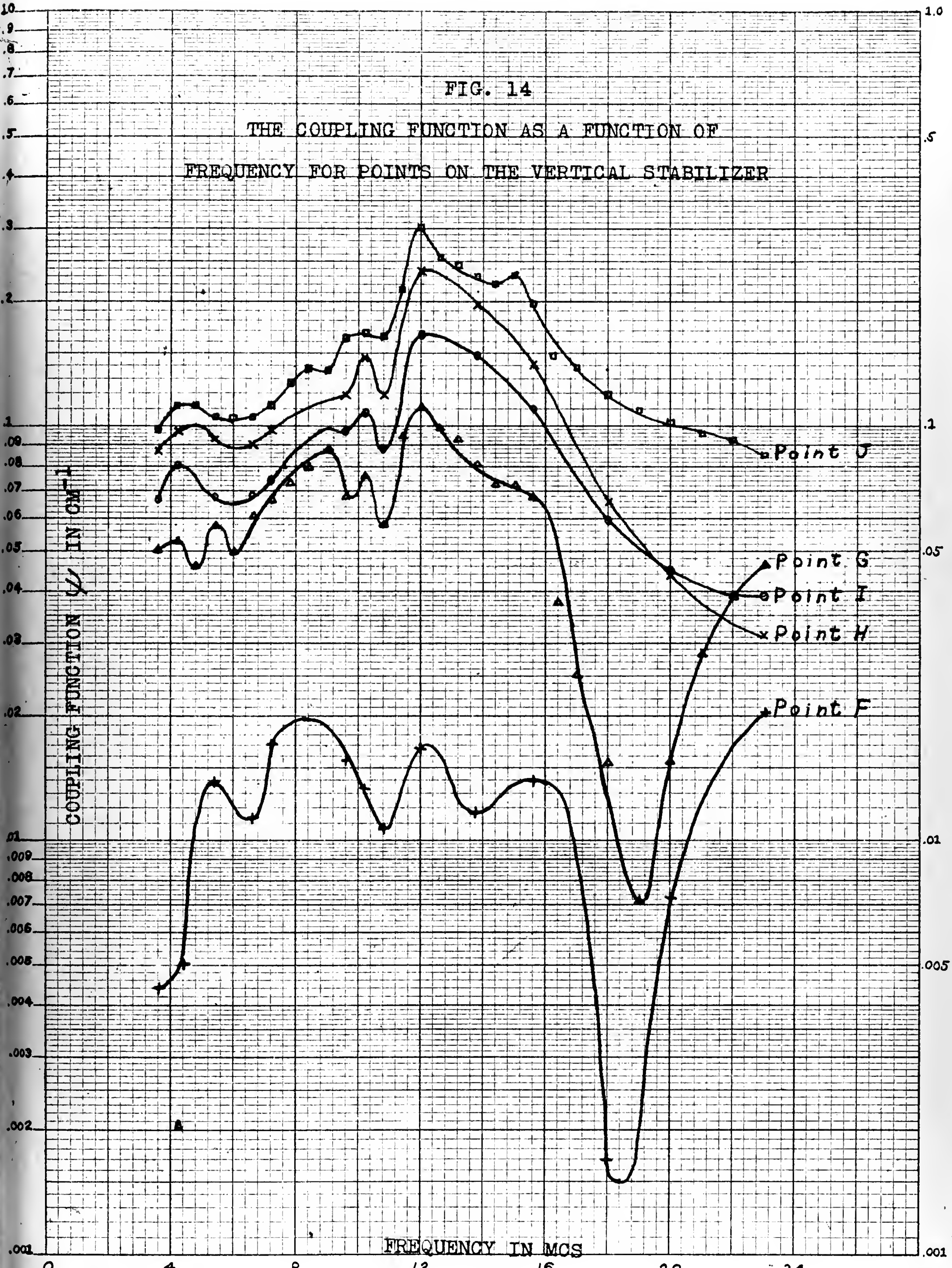
FIG. 14
THE COUPLING FUNCTION AS A FUNCTION OF
FREQUENCY FOR POINTS ON THE VERTICAL STABILIZER
COUPLING FUNCTION ψ IN CM⁻¹
FREQUENCY IN MCS
Point J
Point G
Point I
Point H
Point F
1.0
.5
.1
.05
.01
.005
.001
0
4
8
12
16
20
24

with only small peaks at the frequencies at which the longer element is a integral number of half wave lengths. The coupling for the points on the tail cap can be seen to be much more constant than for other points on the structure. The peak at 12 mc is possibly due to half wave resonance to the nose section. Point G, which is on the lower tail section forming the antenna terminals, would be expected to be similar to point H which is on the antenna terminal on the tail cap. The similarity can be seen with the exception of the low coupling at about 19 mc for point G. This is most probably the low coupling to be expected at $1\frac{1}{4}$ wave lengths for the long element of the antenna. This however, immediately raises the question as to why there is not a similar trough at the 3/4 wave length frequency of 10.5 mcs. This could be caused by some half wave resonance masking the dip at 10.5 mcs and this naturally would not affect the dip at 19 mcs.

Figs. 15 and 16 illustrate the coupling for the points on the wing. Again the half wave and full wave length points can be seen at 7.5 and 15 mcs with the nose section resonance point at 12 mcs. For the points on the outer wing section the $1\frac{1}{4}$ wave length resonance again appears at 18 mcs, while for point K near the wing root the 3/4 wave length minimum coupling becomes pronounced.

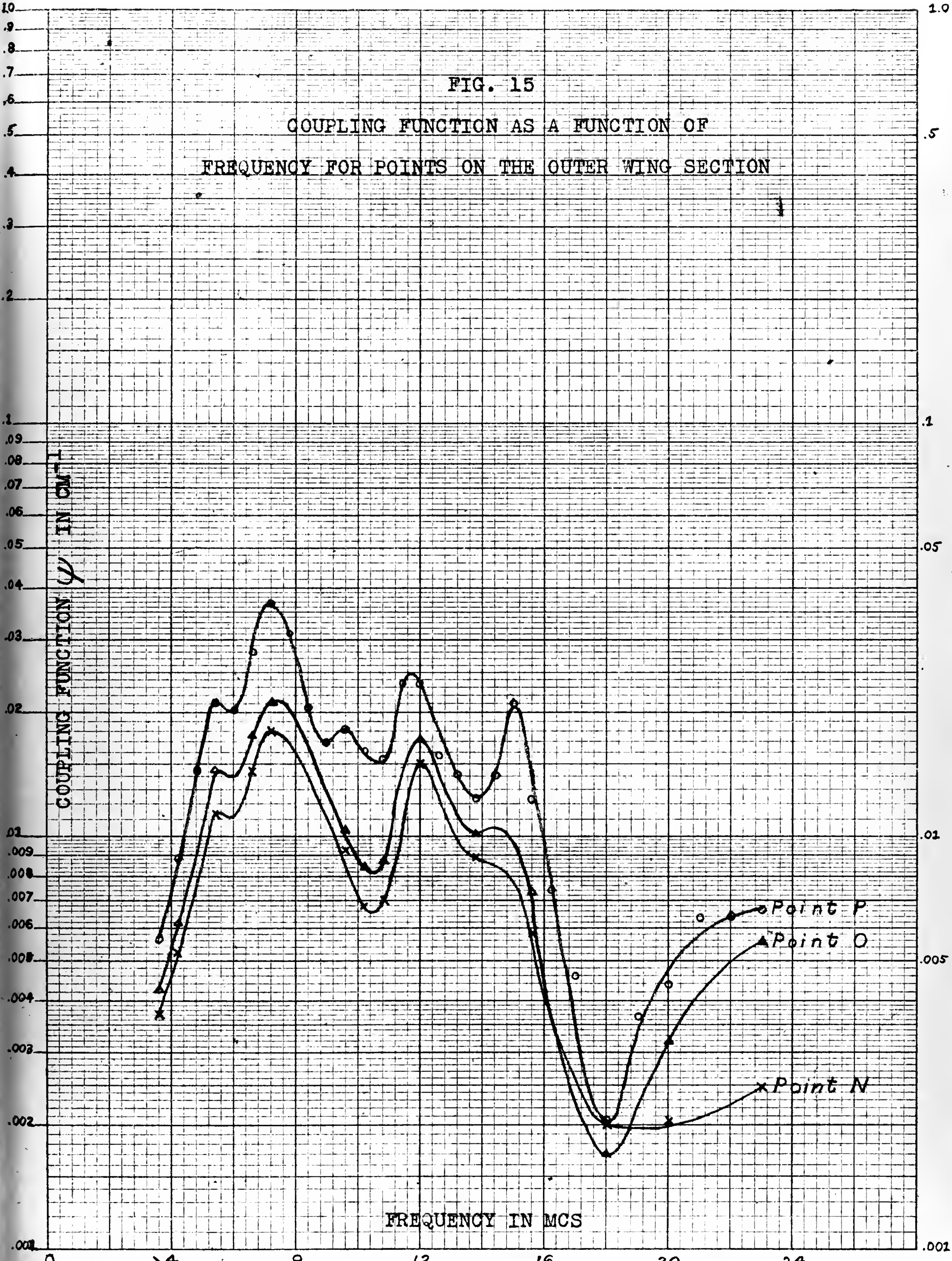

FIG. 15
COUPLING FUNCTION AS A FUNCTION OF
FREQUENCY FOR POINTS ON THE OUTER WING SECTION
COUPLING FUNCTION ψ IN CM^{-1}
FREQUENCY IN MCS
Point P
Point O
Point N
1.0
.9
.8
.7
.6
.5
.4
.3
.2
.1
.09
.08
.07
.06
.05
.04
.03
.02
.01
.009
.008
.007
.006
.005
.004
.003
.002
.001
0
4
8
12
16
20
24

FIG. 16

COUPLING FUNCTION AS A FUNCTION OF FREQUENCY

FOR POINTS ON THE INNER WING SECTION AND JET POD

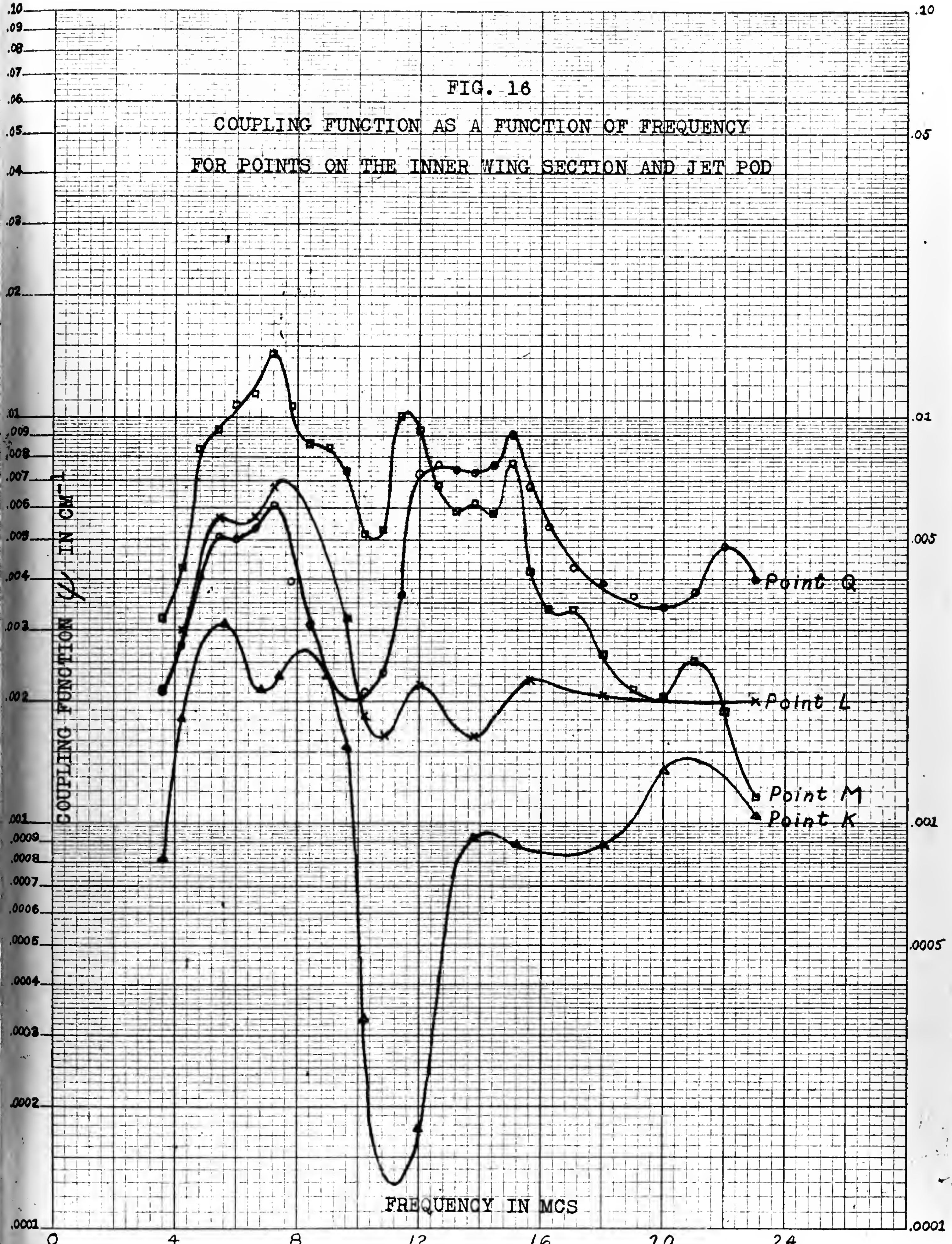

For the wing again as for the tail the similarity of the variation of coupling for the different points can be seen. The difference in coupling between the wing tip and the wing root is quite pronounced, being on the average different by a factor of twenty or more.

In making comparisons between the aircraft and the asymmetric dipole coupling, the similarities are notable, however, the differences also are of note and show that the asymmetric dipole cannot be used as a fairly exact mathematical model. For the asymmetric dipole the first half wave peak for coupling from the end of the longer element is only greater than the quasi-static case by a factor of four. For the measurements made on the aircraft model at the wing tip, the difference between the peak and the lowest frequency measured was a factor of seven.

For the receiver used the lowest frequency available with an extra tuning coil constructed was 18 mcs corresponding to an actual frequency of 3.6 mcs. At this frequency the coupling still appeared to be decreasing with frequency. It would be of interest to know if this were due to a minimum coupling at a quarter wave length and then increased again in the quasi-static region.

In Fig. 17 a comparison of the points of most probable discharge at the extremities of the wing and

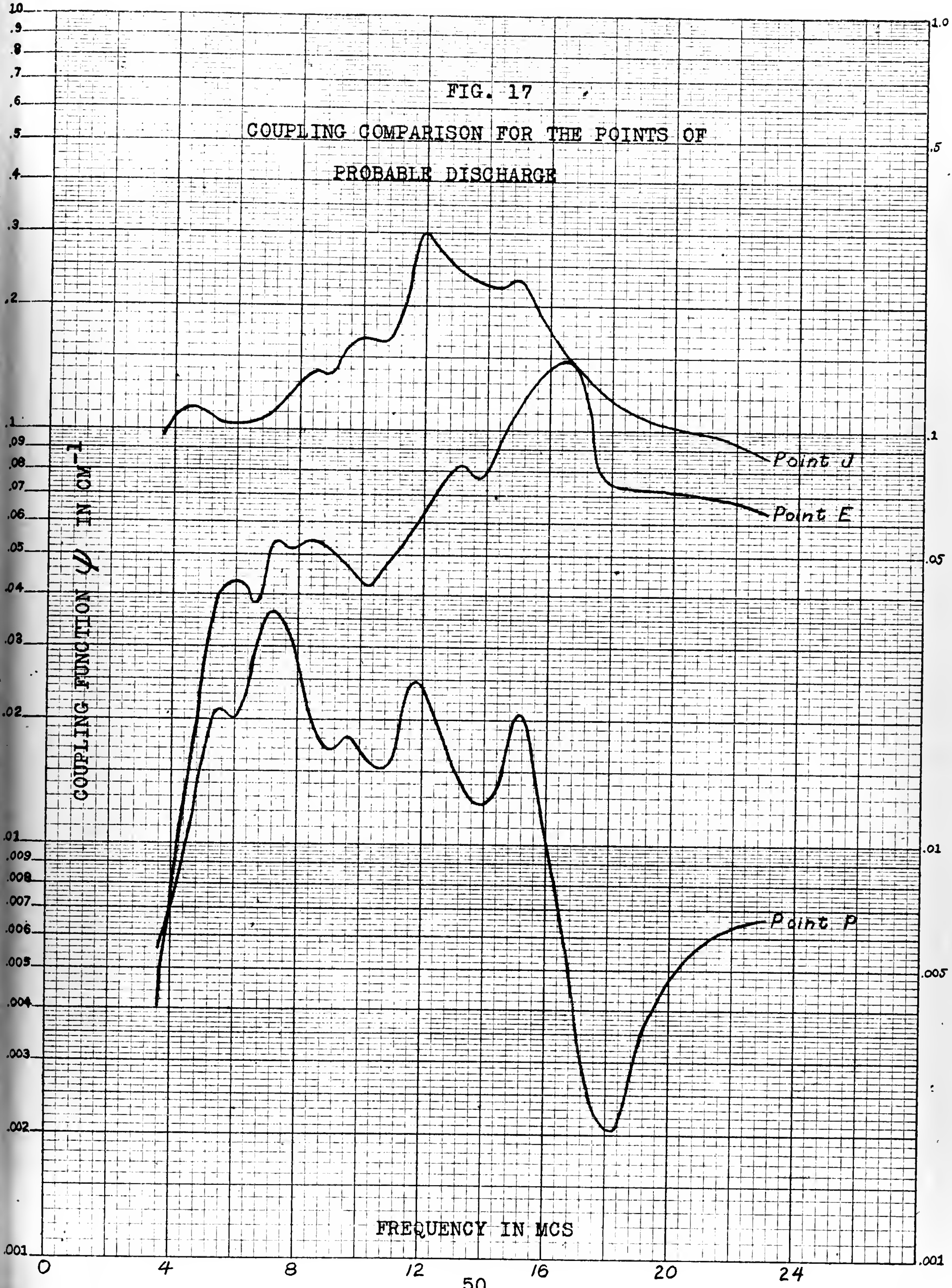
FIG. 17
COUPLING COMPARISON FOR THE POINTS OF
PROBABLE DISCHARGE
COUPLING FUNCTION ψ IN CM^{-1}
FREQUENCY IN MCS
Point J
Point E
Point P
10
.9
.8
.7
.6
.5
.4
.3
.2
.1
.09
.08
.07
.06
.05
.04
.03
.02
.01
.009
.008
.007
.006
.005
.004
.003
.002
.001
1.0
.5
.1
.05
.01
.005
.001
0
4
8
12
16
20
24

tail is made. As can be seen there are no frequencies at which the coupling from all three points is a minimum. The coupling from the wing tip appears to be quite significantly lower than that from the extremities of the tail surfaces. If the discharge could be forced to occur at the wing tip rather than at the other points, the precipitation static noise in the receiver would be quite considerably reduced.

While the tail cap antenna has been very common in modern high speed aircraft, the straight wire antenna is still of interest. A straight wire antenna was connected from an insulator at the top of the vertical stabilizer to antenna terminal points at the midpoint of the wing. The coupling relationship previously derived still hold since basically there is still a single body with a volume removed to form the antenna terminals. In this case one element is the straight wire and the other element is the aircraft itself. The length of wire will now enter into resonance effects causing the maxima and minima coupling frequencies to differ somewhat from those observed for the tail cap antenna.

In Fig. 18 the values of coupling factor for the extremities of the tail surfaces are plotted. It can be seen that the coupling curves are very similar as would be expected since they are now simply two points

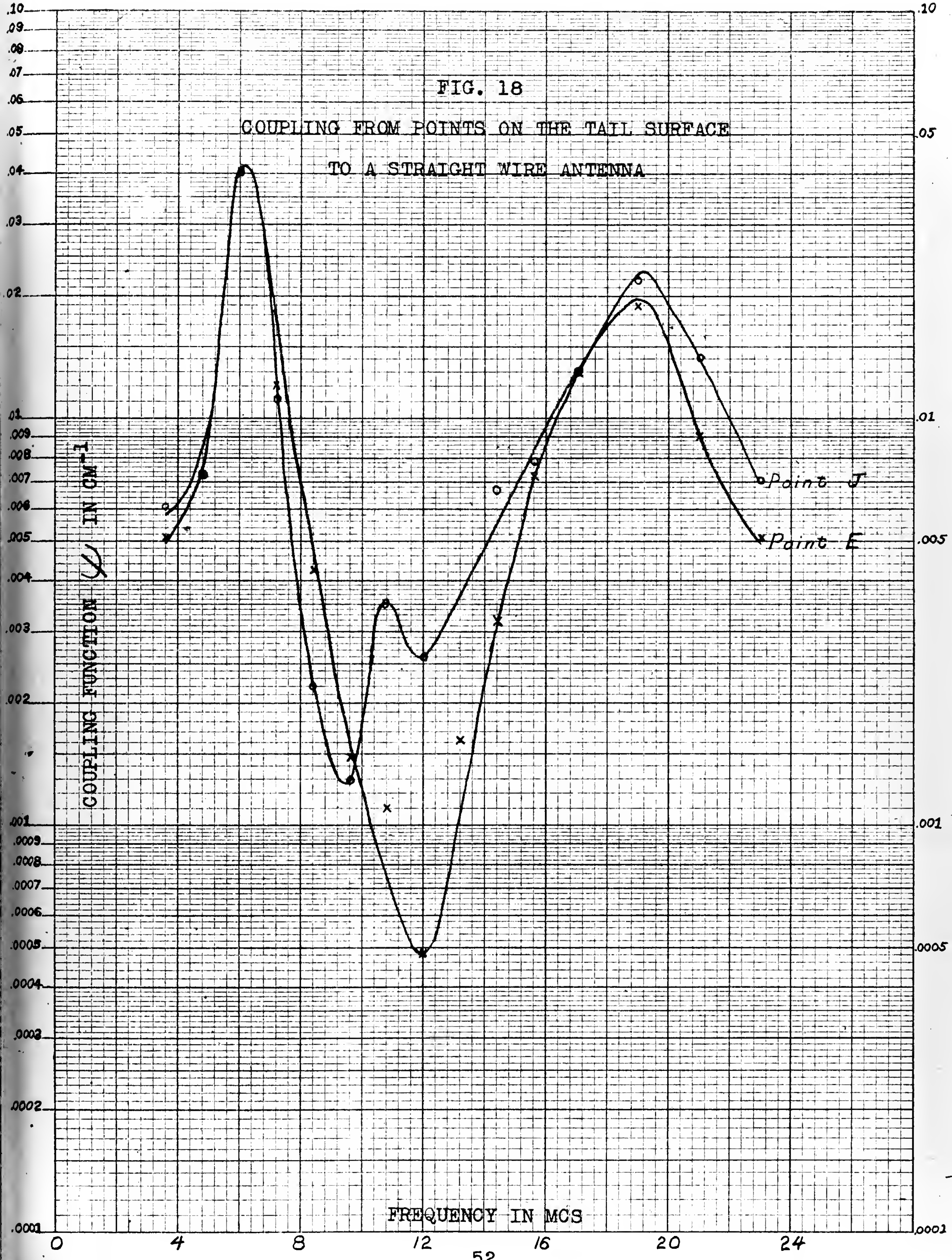
FIG. 18
COUPLING FROM POINTS ON THE TAIL SURFACE
TO A STRAIGHT WIRE ANTENNA
COUPLING FUNCTION (ψ) IN CM^{-1}
FREQUENCY IN MCS
Point J
Point E
.10
.09
.08
.07
.06
.05
.04
.03
.02
.01
.009
.008
.007
.006
.005
.004
.003
.002
.001
.0009
.0008
.0007
.0006
.0005
.0004
.0003
.0002
.0001
0
4
8
12
16
20
24

on similarly shaped extremities at about the same distance from the antenna terminals.

In Fig. 19 coupling is plotted for the wing tip, wing root, and a mid point on the wing. Again the resonant peaks can be seen to occur at the same frequencies for the different points. For the straight wire there is not the extreme difference of coupling between the wing root and the wing tip that was noticed for the tail cap. This is quite possibly caused by proximity of point K to the straight wire antenna terminals.

Coupling from the wing tip and the horizontal stabilizer tip are compared in Fig. 20. The two points can be seen to be quite similar, and therefore coupling from the three most probable discharge points is quite similar. For this type antenna it can be seen that the precipitation static noise can be reduced quite considerably by choice of frequency. The noise in the band from 10-14 mcs would average approximately 20 db less than in the region of 6 mcs.

Figs. 21 through 24 compare the coupling for several points to the tail cap and straight wire. In general it can be concluded that more noise will be generated in the tail cap than in the straight wire antenna since the coupling from the tail section extremities is much greater for the tail cap than for

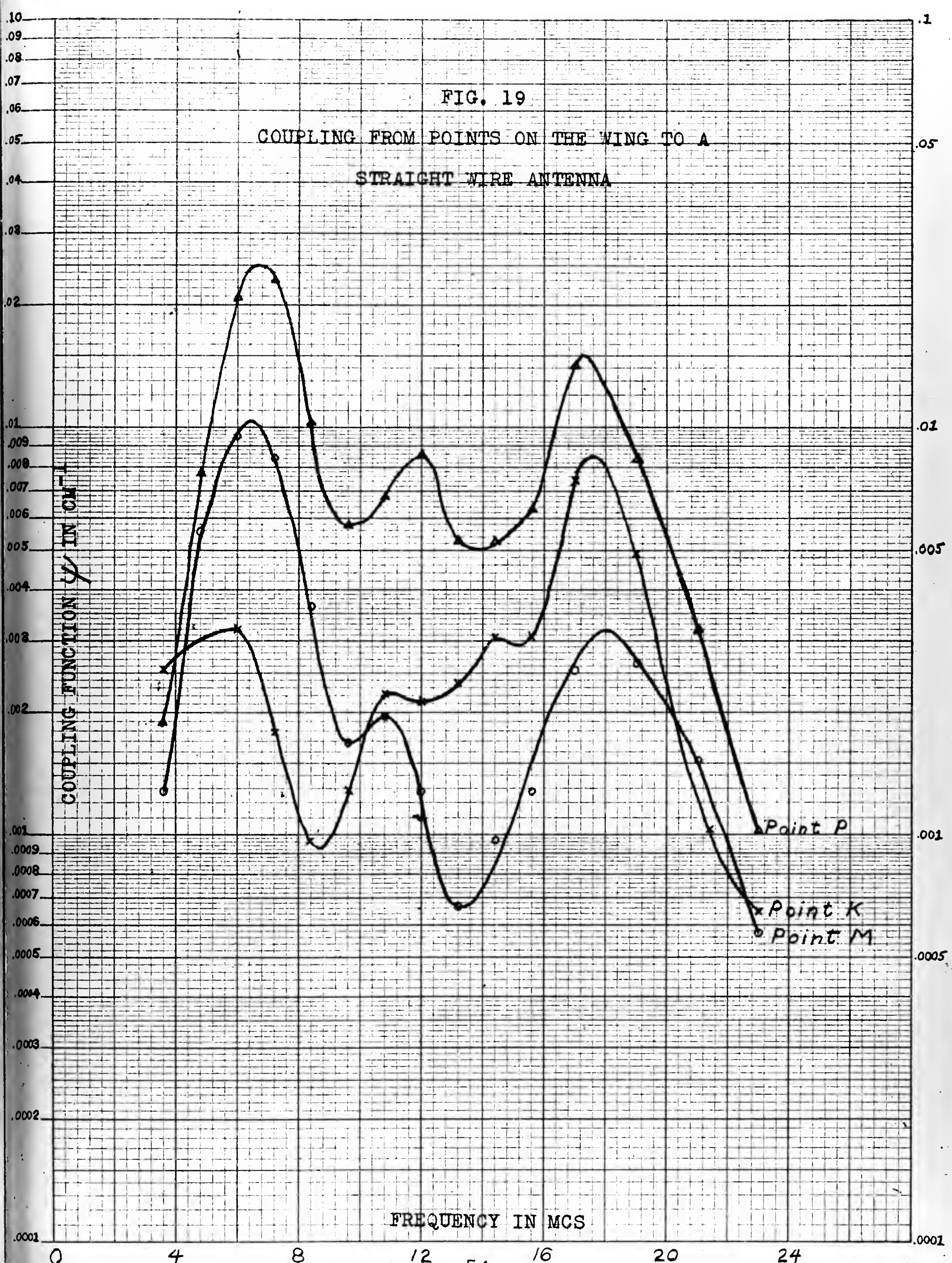
FIG. 19
COUPLING FROM POINTS ON THE WING TO A
STRAIGHT WIRE ANTENNA
COUPLING FUNCTION ψ IN CM^{-1}
FREQUENCY IN MCS
Point P
Point K
Point M
.10
.09
.08
.07
.06
.05
.04
.03
.02
.01
.009
.008
.007
.006
.005
.004
.003
.002
.001
.0009
.0008
.0007
.0006
.0005
.0004
.0003
.0002
.0001
.1
.05
.01
.005
.001
.0005
.0001
0
4
8
12
16
20
24

FIG. 20

COMPARISON OF COUPLING TO A STRAIGHT WIRE ANTENNA FROM THE WING AND THE VERTICAL STABILIZER TIPS

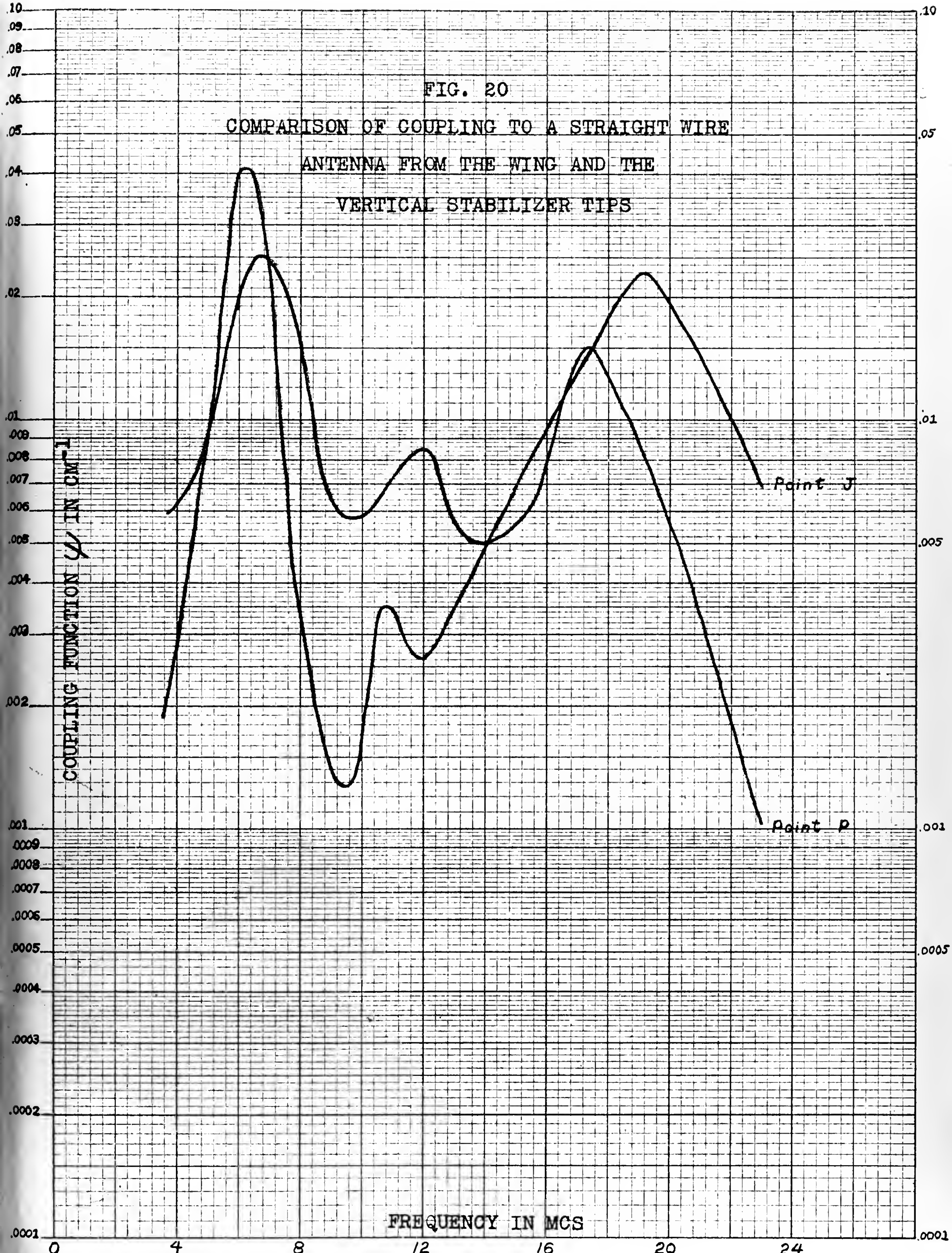

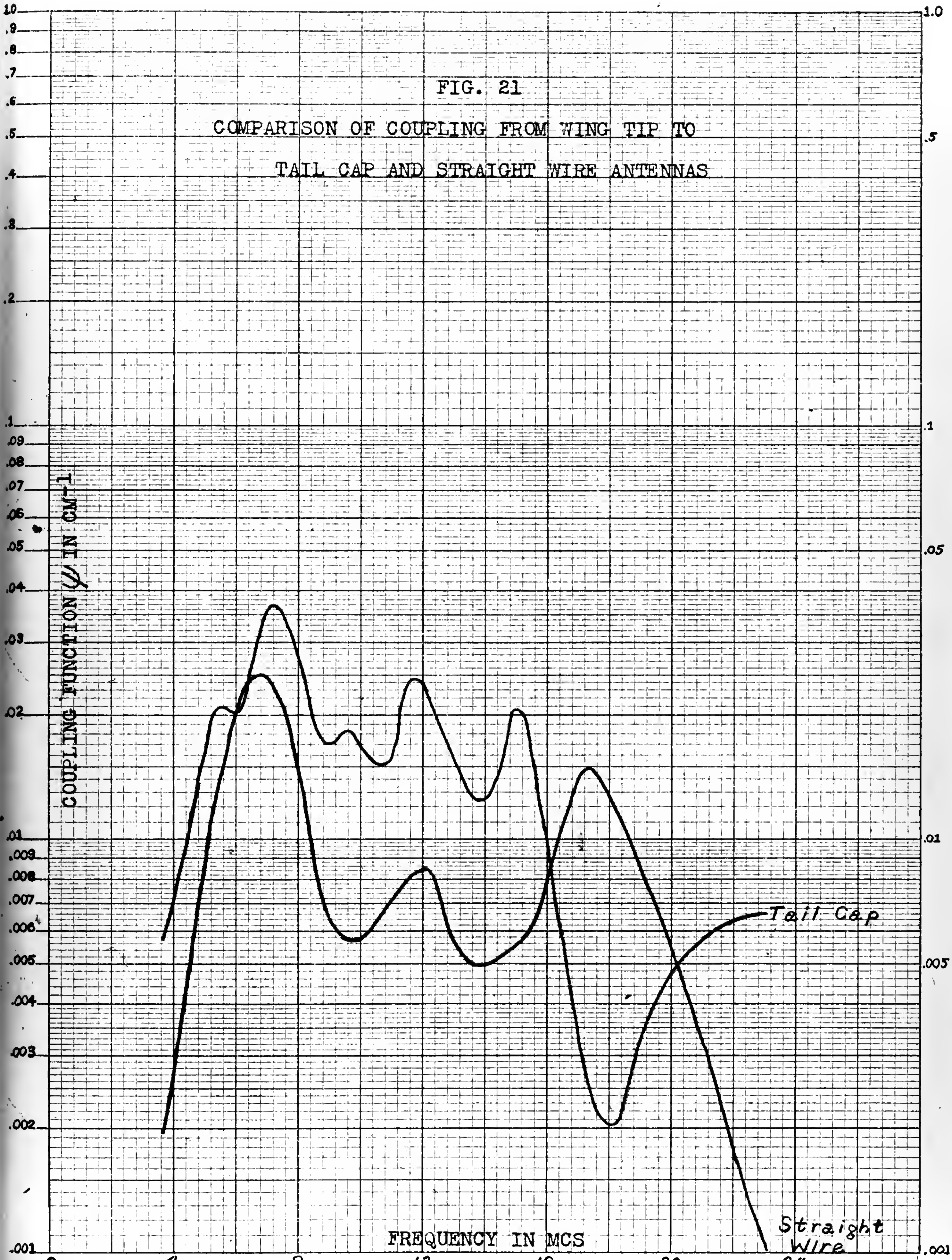
FIG. 21
COMPARISON OF COUPLING FROM WING TIP TO
TAIL CAP AND STRAIGHT WIRE ANTENNAS
COUPLING FUNCTION ψ IN CM-1
FREQUENCY IN MCS
Tail Cap
Straight Wire
1.0
.9
.8
.7
.6
.5
.4
.3
.2
.1
.09
.08
.07
.06
.05
.04
.03
.02
.01
.009
.008
.007
.006
.005
.004
.003
.002
.001
0
4
8
12
16
20
24

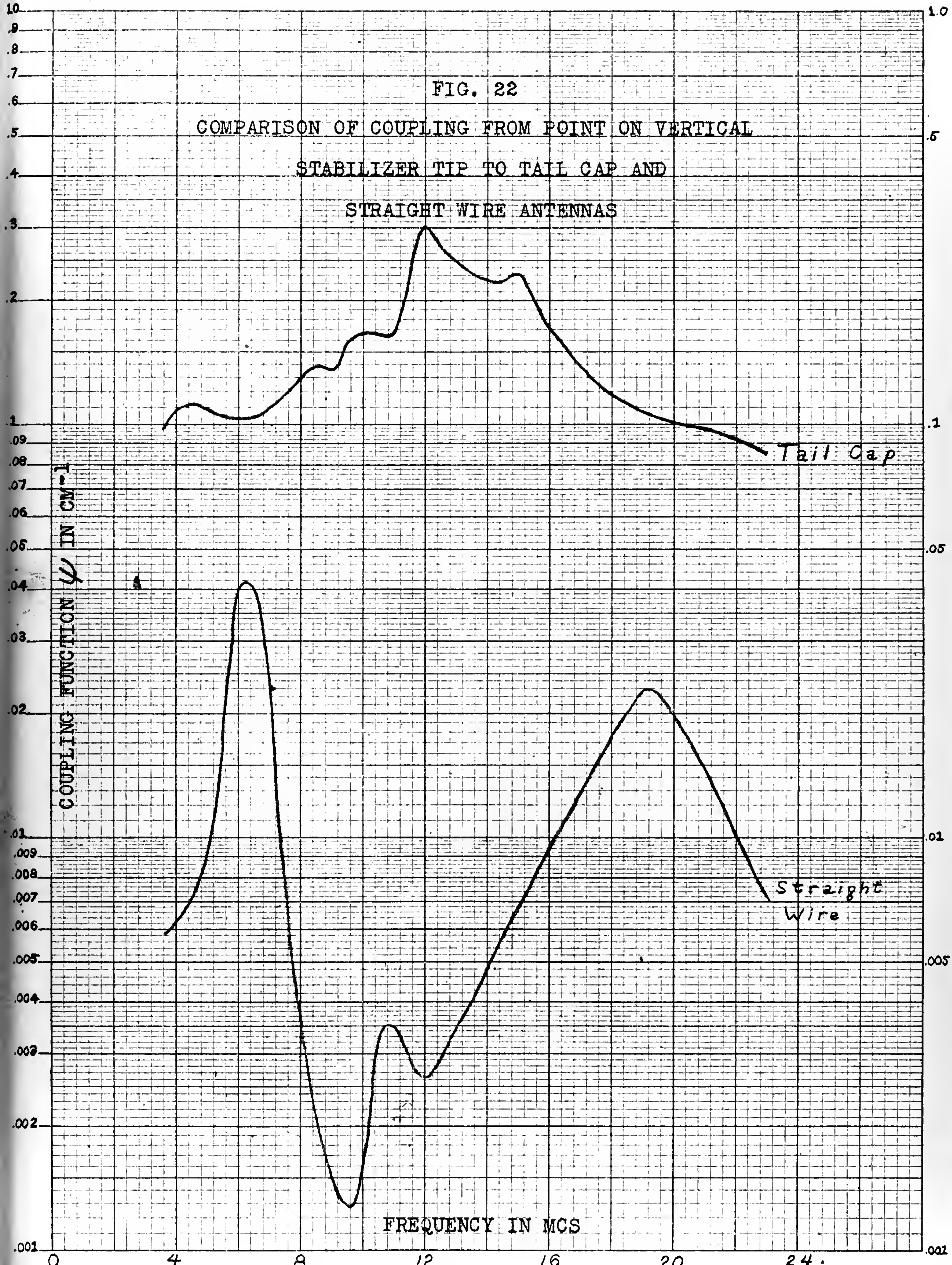
FIG. 22
COMPARISON OF COUPLING FROM POINT ON VERTICAL
STABILIZER TIP TO TAIL CAP AND
STRAIGHT WIRE ANTENNAS
COUPLING FUNCTION ψ IN CM⁻¹
FREQUENCY IN MCS
Tail Cap
Straight Wire
0
4
8
12
16
20
24
1.0
.5
.1
.05
.01
.005
.001

FIG. 23

COMPARISON OF COUPLING FROM HORIZONTAL STABILIZER TIP TO TAIL CAP AND STRAIGHT WIRE ANTENNAS

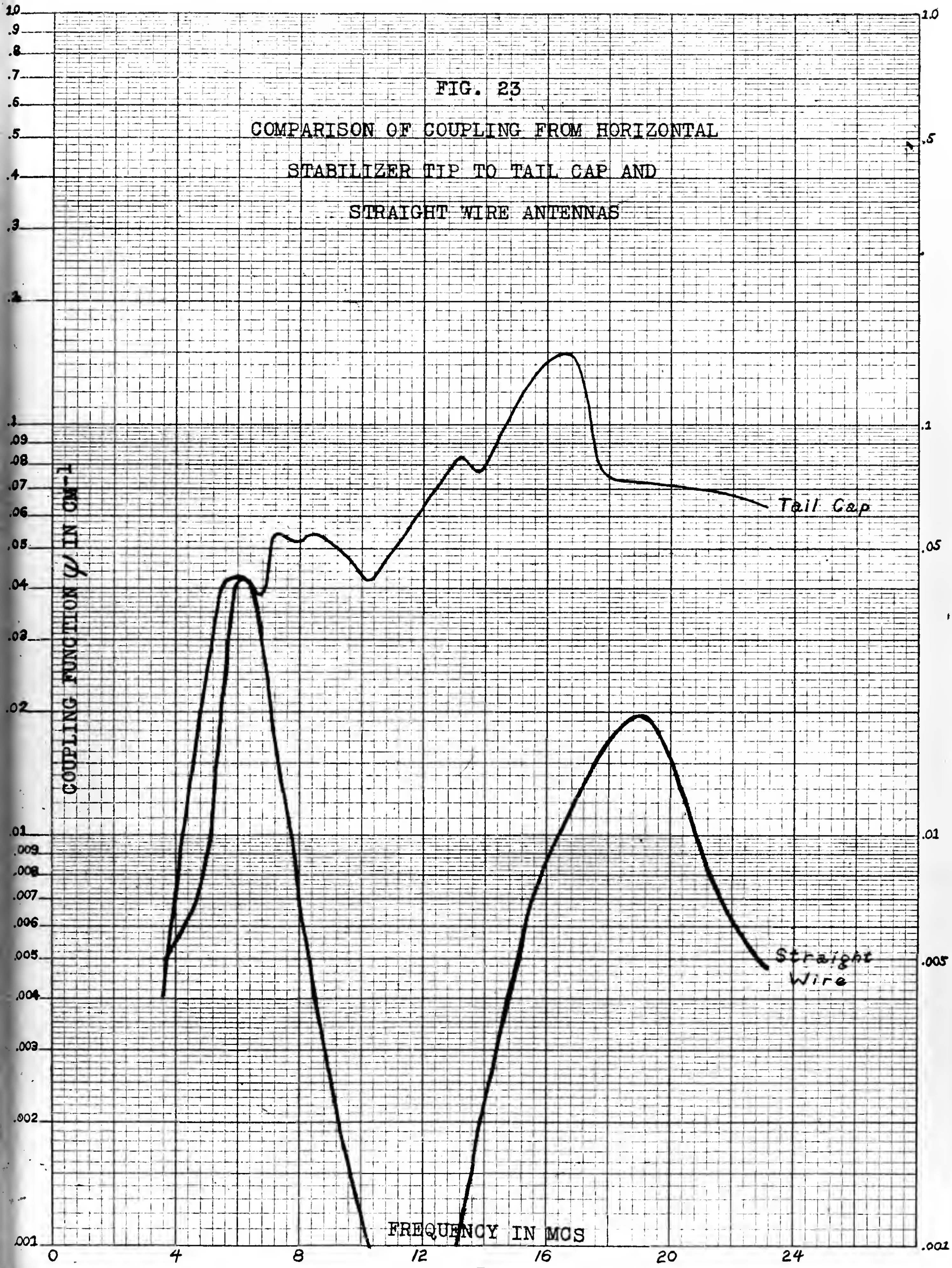

FIG. 24

COMPARISON OF COUPLING FROM A POINT NEAR WING ROOT TO STRAIGHT WIRE AND TAIL CAP ANTENNAS

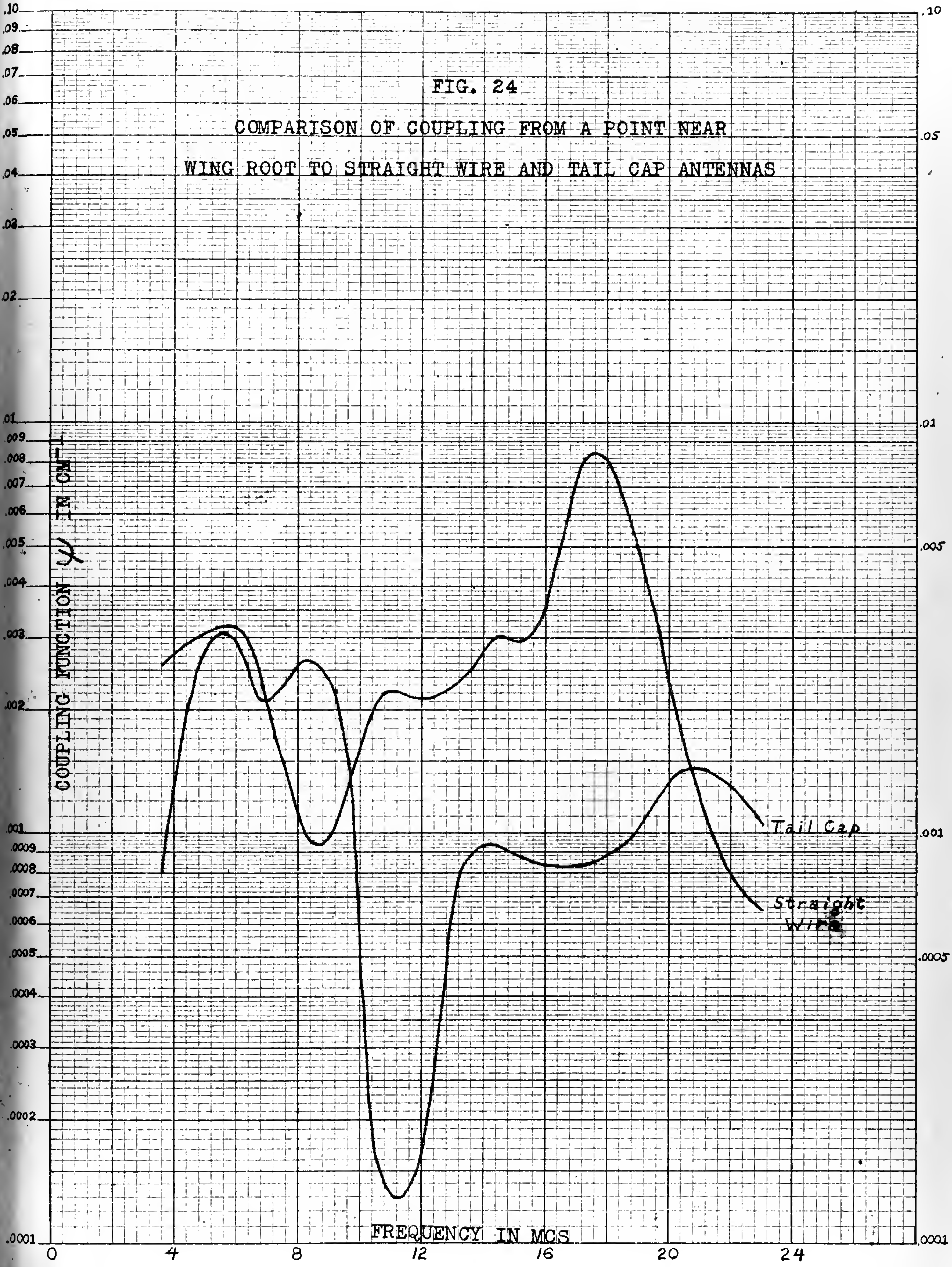

the straight wire while the coupling for the wing tip is approximately the same.

CHAPTER V

CONCLUSIONS

The system devised for measuring the coupling factor worked extremely well. Since the only requirement for the system was that the gain of the receiver and the signal strength remain constant for the period of about 15 minutes required to take readings for a set of points at one frequency, and since there was no need to know the signal strength or gain of the system; simple components could be used for the system and fairly accurate results obtained.

Two sets of readings were taken several days apart with different values of receiver gain and high voltage supply. The difference in coupling factor was on the average less than one db. Some of the points on the curves which appeared as though they might be in error were rechecked and found to correspond almost exactly except in a few cases where apparent errors were discovered. The mirror symmetry obtained for points on the port and starboard horizontal stabilizers also serves to confirm the system accuracy.

The only source of difficulty in the system was in the signal source, since it had to be dismantled and the ball bearing electrodes cleaned and polished after several hours of operation. The signal source

[illegible]

would then be unstable for a period of approximately half an hour while a light oxidation coat built up, and it would then be stable until the oxidation became too great. This could easily be rectified however, either by sealing the gap with a non-corrosive gas in place of the air in the gap, or by making the electrodes of some non-corrosive material.

Study of the curves of coupling function leads to several readily obvious conclusions. For the tail cap antenna it appears that the largest noise source is from discharge on the tail cap itself and that if this could be prevented considerable improvement would be expected at the lower frequencies.

This could be extended further to prevent discharge at the tips of the wing and horizontal stabilizer, and having it occur at a point of low coupling such as the wing root.

The problem now appears to be how to get the discharge to occur at this point without increasing the coupling. This could be done by placing a high negative d.c. potential on some type of discharger such as a wick, so that discharge would occur there before it would discharge at the wing tip or some other high coupling point. By causing the discharge at a naturally low coupling point and also taking advantage of the frequency region of lowest coupling for that point for communications,

the precipitation static noise should be reduced far below that presently encountered with dischargers located at high coupling points.

The measurements made for the straight wire antenna show that from the view point of precipitation static, this type antenna is much more satisfactory than the tail cap. The coupling from points on the tail surface is much lower than for the corresponding points for the tail cap, and it has the additional advantage of a minimum coupling from the normal discharge points at approximately the same frequency.

The problem of precipitation static is still far from being solved. There remains the problem of designing a more efficient discharger that can be located at a low coupling point, or that discharges with smaller amplitude pulses at a higher repetition frequency, or possibly a combination of the two.

BIBLIOGRAPHY

1. R. H. Marriot: "Radio Range Variation," Proc. IRE, Vol. 2, No. 3, March 1914

2. RADM Bruce McCandless; "St. Elmo's Fire," U.S. Naval Institute Proc., Vol. 83, No. 2, February 1957

3. A. Curtis: "Discussion on Radio Range Variation by R. H. Marriot," Proc. IRE, Vol. 2, No. 3, March 1914

4. H. W. Morgan: "Rain Static," Proc. IRE, Vol. 24, No. 7, July 1937

5. H. M. Hucke: "Precipitation Static Interference," Proc. IRE, Vol. 27, No. 5, May 1939.

6. Ross Gunn et al: "Army-Navy Precipitation Static Project," Parts I - VI, Proc. IRE, Vol. 37, Nos. 4 and 5, April and May 1956

7. W. H. Huggins, "Final Report on Precipitation Static Reduction Research, June 15, 1941 - March 31, 1943," Oregon State College.

8. I. Langmiuir, "Final Report on Investigation of Fundamental Phenomena of Precipitation Static," Report on Contract No. W-33-106-5C-65, General Electric Co., May 1945

9. I. Langmuir, and H. E. Tanis, "The Electrical Charging of Surfaces Produced by the Impact of High Velocity Solid Particles," Report on Contract No. W-33-106-5C-65, General Electric Co., May 1945.

10. H. J. Dana "Block and Squirter for Reduction of Precipitation Static," Second Air Force Operations Analysis Report No. 15, February 1945.

11. Willard H. Bennett, "Snow Static on Aircraft," Electrical Engineering, Vol. 67, Oct. 1948

12. R. Beach, "Electrostatic Ills and Cures of Aircraft," Electrical Engineering, Vol. 66, Oct. 1947

13. Philco Corp., Research Div., "Final Engineering Report on Precipitation Static Reduction," U.S.A.F. Contract No. W33-038ac20763, February 9, 1950.

14. "Limitations on the Design of a Practical Ionic Static Discharger," AMC Engineering Memo Report MCREE-50-30, 2 June 1950.

15. Cornell Aeronautical Laboratory, "Investigation of Means to Maintain Zero Electrical Charge on Aircraft." Final Report, Contract No. AE19(122)-475, October 31, 1953.

16. R. L. Tanner, "Radio Interference from Corona Discharges," Tech. Report No. 37, SRI Project No. 591, U.S.A.F. Contract No. AF19(604)-266, April 1953, Stanford Research Institute.

17. Denver Research Institute, "Development of Aircraft Discharge Methods," Final Report Contract No. AF33(616)-157, April, 1956

18. R. L. Tanner and J. E. Nanevicz, "Radio Noise Generated on Aircraft Surfaces" Contract No. AF33(616)-2761, September 1956, Stanford Research Institute.

19. M. M. Newman and J. L. Rondiau, "Radio Interference from Charged Rain Drops." Abstracts of papers delivered at 1952 Conference on Airborne Electronics.

20. J. A. Stratton, Electromagnetic Theory pp. 485-486 McGraw-Hill Book Co., Inc. New York, 1941.

21. L. B. Loeb, Fundamental Processes of Electrical Discharge in Gases, John Wiley and Sons, Inc.,

22. L. B. Loeb and J. M. Meek, The Mechanism of the Electric Spark, Stanford University Press, Stanford University, California, 1941.

JA 17 BINDERY

Thesis
J477 Jesse 35713
Coupling from points on
an aircraft structure to
aircraft antenna terminals
JA 17 58 BINDERY

Thesis
J477 Jesse 35713
Coupling from points on an aircraft structure to aircraft antenna terminals.